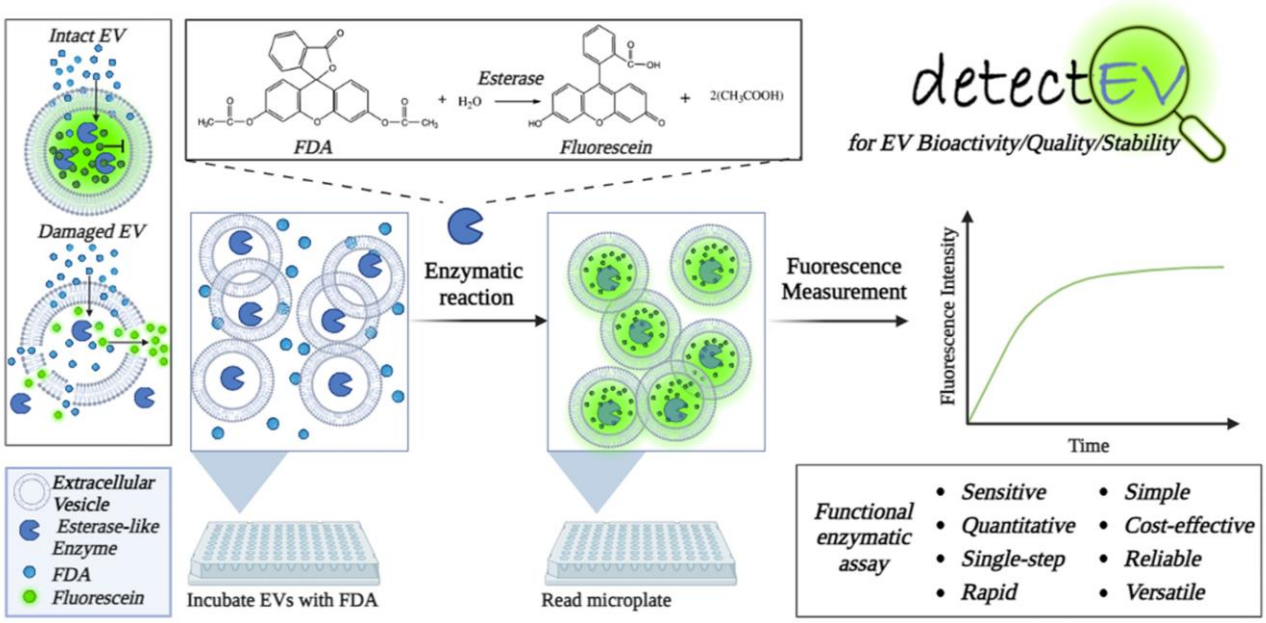
Intact EV
Damaged EV
Esterase
FDA
Fluorescein
detectEV
for EV Bioactivity/Quality/Stability
Enzymatic reaction
Fuorescence Measurement
Fluorescence Intensity
Time
Extracellular Vesicle
Esterase-like Enzyme
FDA
Fluorescein
Incubate EVs with FDA
Read microplate
Functional enzymatic assay
Sensitive
Quantitative
Single-step
Rapid
Simple
Cost-effective
Reliable
Versatile

DetectEV: a functional enzymatic assays to predict the potency of extracellular vesicles

Giorgia Adamo,[*a] Sabrina Picciotto,[a] Paola Gargano,[a] Angela Paterna,[b] Samuele Raccosta,[b] Estella Rao,[b] Daniele Paolo Romancino,[a] Giulio Ghersi,[c] Mauro Manno,[b] Monica Salamone [a], and Antonella Bongiovanni.[*a]

a. Cell-Tech HUB and Institute for Research and Biomedical Innovation (IRIB), National Research Council of Italy (CNR), Palermo 90146, Italy.

b. Cell-Tech HUB and Institute of Biophysics (IBF) - CNR, Via Ugo La Malfa 153, 90146 Palermo, Italy.

c. Department of Biological, Chemical and Pharmaceutical Sciences and Technologies (STEBICEF), University of Palermo, 90128 Palermo, Italy.

Giargia Adamo and Sabrina Piciotto contributed equally to this work.

Corresponding Authors: *giorgia.adamo@irib.cnr.it; *antonella.bongiovanni@irib.cnr.it.

The applications of extracellular vesicles (EVs) as therapeutics or nanocarriers for cell-free therapies necessitates a comprehensive assessment of their bioactivity, batch-to-batch reproducibility, and stability. Due to the considerable heterogeneity in EV preparations, there is a crucial need for a sensitive functional test to complement established methods for EV characterization.

In this study, we introduce the detectEVs assay, an enzymatic-based approach designed to evaluate EV bioactivity. Specifically, this assay enables quantitative measurement of both EV bioactivity and integrity in small-size EV samples through a single-step analysis. Moreover, the detectEV assay proves effective for quality checking EVs post-isolation, during storage, and loading processes. The development and validation of this robust and straightforward test were extended to EVs from different cell lines and hold promise for enhancing the characterization of EVs, thereby enabling the prediction of their potency.

Keywords: extracellular vesicles, integrity, bioactivity, functional enzymatic assay, potency, quality, standardization.

Introduction

Extracellular vesicles (EVs) are essential signalling mediators involved in intercellular and inter-organism communications (Adamo et al., 2021; Raposo et al., 2013; Yáñez-Mó et al., 2015) . EV-based signaling rely on their cargo, which can be naturally-sourced (bioactive molecules such as RNAs or enzymes), or exogenously loaded (e.g., RNAs or drugs) (Y. Chen et al., 2021; O'Grady et al., 2022). In recent years, EVs have come to be considered one of the most promising innate effectors for cell-free therapy and bio-nanovehicles for drug delivery (Herrmann et al., 2021). However, despite the advances in the field, many challenges with EV-based therapies still stand. The problem with human cell-derived EVs lies in their inherent variability, stemming from differences in input materials (i.e., donor cells). This variability has implications for safety and scalability of the EV production process (Sun et al., 2021). The therapeutic efficacy of EVs depends on a variety of additional parameters, some of which can be addressed only during laborious and expensive preclinical trials (Nguyen et al., 2020). To validate the quality of EV preparations and define the "Critical Quality Attributes" (CQA), EV-inherent features should be tested to qualify them as suitable for subsequent clinical functional testing applications (Yekula et al., 2020). In this view, to achieve an adequate assessment of EV bioactivity, appropriate functional assays need to be created to support common EV-related biophysical and biochemical quality controls (QCs).

Ideally, specific functional assays would predict whether a particular EV-preparation holds the potential to achieve its intended therapeutic effects, which could be further investigated in a "formal disease-specific" potency assays (Nguyen et al., 2020; Bruno et al., 2017).

The MISEV-2023 guidelines and the EV-TRACK knowledgebase propose and support rigorous procedures required to document specific EV-associated functional activities to cope with the advance of EV research, assuring and improving the quality of these studies (Welsh et al., 2024; Van Deun et al., 2017). In particular, the MISEV-2023 recommendations for conducting functional studies encourage researchers to conduct dose-response and time-course studies, incorporate EV-negative controls, utilize EVs from different cell types for comparative analysis, and employ treated-EV samples to differentiate EV-specific effects from co-isolating materials. Moreover, it is suggested to explore the impact of EV separation or storage methods on EV activity to optimize experimental conditions (Welsh et al., 2024).

Furthermore, a functional assay should be simple and sensitive enough using a low amount of EV samples to facilitate the following studies (Pachler et al., 2017; Gimona et al., 2021). To date, only few *in vitro* and *in vivo* assays have been used to interrogate the potency of specific types of EVs; however, many of them failed for several challenges that make reliable assays difficult to set up

(Nguyen et al., 2020; Ramirez et al., 2018). In the field of extracellular vesicles, it is expected that no single test can adequately measure all product attributes that can predict clinical efficacy. Further, the development of ubiquitous, standardisable and functional test for evaluating the bioactivity can be tricky for EVs because they are highly heterogeneous and show different functional activities (Zheng et al., 2023). Despite this evidence, there is a need for a precise procedure to accurately qualify EV preparations, which can be applied to various types of EVs, regardless of their origin or preparation method (Gimona et al., 2021). It would be advisable to identify a common feature among vesicles that could provide a general indication of their biological activity. An example could be measuring enzymatic activity by identifying a class of enzymes ubiquitously present in extracellular vesicles. In this context, a fascinating and unexplored aspect is the presence of esterases within EVs. A search on the publicly available ExoCarta database revelled a noticeable and extremely robust association between esterase-like enzymes and vesicle-cargo proteins in EVs derived from many sources, including ones of mammalian origin (mice, rats, and cows), several human body fluids (blood, saliva, and urine) and numerous human cancer and normal cell lines (more than 60 hits for "esterase" from the ExoCarta database, http://www.exocarta.org) (Gonzalez-Begne et al., 2009; Gonzales et al., 2009; Simpson et al., 2012). Furthermore, many recent proteomic analyses described the presence of esterase-like enzymes in EVs isolated from bacteria (like *Escherichia coli* and *Pseudomonas aeruginosa*), plants and fungi (*Candida albicans* and *Aspergillus fumigatus*) (Pocsfalvi et al., 2018; Rizzo et al., 2020; Choi et al., 2011; Garcia-Ceron et al., 2021; Bleackley et al., 2020; McMillan and Kuehn, 2022). A large number of enzymes, such as choline esterases, carboxylic ester hydrolases, lipases, and proteases, are member of the esterase' superfamily, catalyzing the cleavage of ester bonds (Cygler et al., 1993). The measure of esterase activity can be performed by employing an enzymatic assay, using specific substrate, like the fluorescein diacetate. Fluorescein diacetate (*i.e.* 3'-6'-diacetyl-fluorescein, FDA) is a non-fluorescent fluorescein molecule conjugated to two acetate radicals (Adam and Duncan, 2001). This is a fluorogenic ester compound able to pass through phospholipid bilayers, like plasma and EV membranes. Indeed, when inside cells or EVs, FDA is hydrolyzed by non-specific esterases to produce a negatively charged membrane-impermeable green fluorescent molecule (*i.e.*, fluorescein) (Fontvieille et al., 1992). This membrane-permeable esterase substrate is commonly used as a probe to study microbial metabolic activity or to monitor the cell viability of fungi, plants, microalgae, and bacteria. It can be used both to measure enzymatic activity, essential for activating its fluorescence, and to evaluate membrane integrity, necessary for the intracellular or intra-vesicular retention of its fluorescent product (Ender et al., 2020; Gray et al., 2015; Pospichalova et al., 2015; de Rond et al., 2018).

In the EV-field, different approaches have described the use of membrane-permeant enzymatic substrates to label ~~small~~ EVs, including carboxyfluorescein diacetate-acetoxymethyl ester (CFDA), carboxyfluorescein diacetate succinimidyl ester (CFSE), and calcein acetoxymethyl ester (calcein-AM) (Ender et al., 2020; Nikiforova et al., 2021; Tertel et al., 2022; Kormelink et al., 2016). Similarly to FDA, these molecules are cleaved by enzymes, which are present inside cells as well as in secreted EVs (Gray et al., 2015). These experimental approaches have been developed to make EV fluorescent and detectable for flow cytometry applications or for fluorescent microscopy; however, these methods are not quantitative and do not directly provide information on EV-functional quality (Morales-Kastresana et al., 2017).

In this study, we introduced the detectEV assay as a new, simple, highly sensitive and precise functional test, able to predict the potency of EVs, by contextually evaluating the enzymatic activity and membrane integrity, using an FDA-based enzymatic method (Sırt Çıplak and Akoğlu, 2020; Adam and Duncan, 2001). Throughout this assay, we considered various aspects crucial for working with EVs, as comparing the quality of different EV batches or EVs isolated using different methods (differential ultracentrifugation versus tangential flow filtration). Additionally, we assessed the bioactivity and integrity of EVs stored under different conditions or manipulated using various physical loading techniques, using the proposed functional test and comparing these results with a standard method for EV evaluations, like nanoparticle tracking analysis (Welsh et al., 2024). Finally, we proved that the detectEV assay can predict the potency of different preparations of EVs. The versatility of the detectEV assay for different type of EVs, including human ones, encouraged its application as functional enzymatic assay for rapid QC check of EVs, as in a single step analysis giving two important pieces of information: the bioactivity that is related to membrane integrity of EV preparations.

Results

Set up of the detectEV assay

To set up the detectEV assay, we used microalgae-derived extracellular vesicles (called nanoalgosomes or algosomes) as small EV (sEV) models (Adamo et al., 2021). We optimized the renewable/large-scale isolation of nanoalgosomes from the conditioned media of *Tetraselmis chuii* (*T. chuii*) microalgae, using the tangential flow filtration method. Next, we characterized them by evaluating selected MISEV-2023 quality parameters (Adamo et al., 2021; Welsh et al., 2024). These included biophysical characterization of size distribution and morphology by dynamic light scattering

(DLS), nanoparticle tracking analysis (NTA) and atomic force microscopy (AFM), and a biochemical characterization of protein content using bicinchoninic acid assay (BCA assay) and immunoblot (IB) analysis for EV-biomarkers (Adamo et al., 2021; Paterna et al., 2022). Data relative to nanoalgosome characterization are reported in **Supporting Figure 1** (EV-TRACK ID: EV231004). In particular, nanoalgosomes exhibited a monodisperse size distribution of approximately 100 ± 10 nm, a rounded and homogeneous morphology, and the presence of enriched EV biomarkers such as Alix, H+-ATPase, and β-actin. Additionally, they are expected to demonstrate an appropriate EV particle number/protein/particle number ratio, in which 1 µg of total EV protein corresponding to a range of 5-10 x 10^9 particles (Sverdlov, 2012).

In the proof-of-concept of the proposed detectEV assay, the accumulation of fluorescein inside EVs is a measure of two independent parameters: enzymatic activity and membrane integrity (**Figure 1a)**. Therefore, in a first pilot test, we incubated a fixed amount of nanoalgosomes ($2x10^{10}$) with fluorescein diacetate (i.e. 3'-6'-diacetyl-fluorescein, FDA) (35 µmol) in 200µl of phosphate saline buffer solution (PBS) and checked for fluorescence emission with respect to EV-negative control (nanoalgosome vehicle solution, *i.e.,* PBS), using spectrofluorometer readings (**Figure 1b**). The fluorescence emission was detected over time, up to 16 hours (960 min). Interestingly, we got a rapid time-dependent increase of fluorescence intensity only in the nanoalgosome samples compared to the negative control. The trend of fluorescence increase over time exhibits a direct proportionality, *i.e.,* a linear relationship up to 8 hours, and subsequently reaches a plateau after approximately 15 hours, probably due to substrate depletion or enzyme inactivation. (**Figure 2**).

Based on this result, fundamental parameters such as the temperature set at 22°C (*i.e.,* room temperature) and the duration of the assay limited to 3 hours (a time frame during which the reaction remains within the exponential phase and exhibits a linear trend) were defined. These parameters were established to ensure the test is rapid and sufficiently sensitive.

Validation of the quantitative FDA-based functional enzymatic assay for EVs

For the validation of the analytical procedure, it is important to establish key parameters such as specificity, accuracy, and precision (Guidance for Industry Potency Tests for Cellular and Gene Therapy Products, 2011). Initially, we gated the appropriate approach to develop a functional assay for EVs that provides a universally quantifiable and standardizable read out. To accomplish that we had to determine the amount of FDA that is enzymatically cleaved during the assay, establishing a calibration curve to interpolate unknown quantities of cleaved FDA. Therefore, the fluorescein, corresponding to the reaction product of FDA hydrolysis, was deemed a reliable choice, and, in turn,

it was generated a standard calibration curve using it (Dzionek et al., 2018). **Figure 3a** illustrates **the calibration curve** derived from serial dilutions of a fluorescein stock solution, where the fluorescence emission intensity exhibits a direct correlation with fluorescein concentration. The resulting calibration curve demonstrates a linear trend, facilitating the straightforward conversion of fluorescence intensity emitted following the enzymatic reactions (*i.e.*, FDA hydrolysis by active EV-related esterases) into nanomole (nmol) of produced fluorescein. Furthermore, in the development of the detectEV assay, we have chosen to adopt the enzymatic units (U) to quantitatively assess EV-related enzymatic activity. This because the specific enzymatic activity is universally expressed as U, representing the quantity of enzyme required to catalyse the conversion of one nanomole of substrate into product per minute (nmol/min), under the specified conditions of the assay method (Robinson, 2015).

Therefore, within the detectEV setup, enzymatic units (nmol/min) will be determined by utilizing a calibration curve of free fluorescein to calculate the total nmols generated over 180 minutes. Subsequently, total nmols will be divided by the overall time (180 minutes) to yield the final readout in nmol/min.

Additionally, in order to determine kinetic parameters of the enzymatic reaction, we performed an enzymatic kinetic study at increasing substrate concentrations, to measure the reaction rate (*i.e.*, the amount of substrate converted to product per unit of time) at constant nanoalgosome concentrations ($2x10^{10}$ nanoalgosomes). This approach reflects the Michaelis-Menten model, a widely utilized method for studying enzyme kinetics (Bisswanger, 2014; Choi et al., 2017; Michaelis et al., 2011). As shown in **figure 3b**, by plotting reaction rates against the respective substrate concentration, we obtained a canonical hyperbolic relationship, through which it was possible to derive kinetic parameters, including the maximum reaction velocity (Vmax, equal to 2.9 nmol/min) and the kinetic constant (as Michaelis constant, Km equal to 3 µmol) (Michaelis et al., 2011; Duggleby and Wood, 1989).

These values could give an indication on the substrate concentration to be used to ensure that the enzymes are acting near Vmax (Bisswanger, 2014). Typically, a substrate concentration higher than the Km value is employed in enzymatic activity studies (Bisswanger, 2014). Based on this evidence, for establishing the right detectEV assay condition, we decided to fix the substrate concentration (*i.e.*, FDA) at 6 times the Km that is at 18 µmol (Michaelis et al., 2011; Duggleby, 1979).

Analytical sensitivity and specificity of detectEV assay

To establish the **analytical sensitivity** of the detectEV assay, we determined the limit of detection (LOD) by conducting a dose-response test to identify the lowest concentration of EVs that could be distinguished from the background noise. This background noise corresponds to the nanoalgosome buffer control (v/v of PBS solution) incubated with FDA.

Therefore, to determine the LOD, we incubated different nanoalgosome concentrations of the same preparation batch (ranging from $3x10^8$ to 2×10^{10} EVs) with 18 µmol of FDA. We found that the enzymatic assay is EV-dose responsive, with the minimum detection limit of $2x10^9$ nanoalgosomes (**Figure 4a**).

Additionally, to verify whether the **analytical specificity** of the detectEV assay is associated with the bioactivity of active enzymes within intact EVs, we utilized nanoalgosomes treated with varying concentrations of a non-ionic detergent (Triton-X 100 at 0.1%, 0.25%, 0.5%, and 1%). This detergent permeabilizes lipid membrane bilayers and gently solubilizes proteins while maintaining their activity, including enzymatic activity (Perna et al., 2017). As established in our prior study, complete nanoalgosome lysis was induced by treating with 1% Triton-X 100 (Adamo et al., 2021). Subsequently, we performed the detectEV assay using detergent-treated nanoalgosomes respect to not treated ones. The results showed in Figure 4b revealed higher enzymatic activity in the intact/no-treated nanoalgosomes, while this activity decreased with increasing doses of detergent, reaching no activity at the critical detergent concentration of 1%. This suggests that the measurable fluorescent signal relies on active esterases within the physiological environment of intact EVs. Identical results were observed when EVs were lysed, and proteins were denatured by boiling at 100°C for 10 minutes, thereby confirming the specificity of the proposed functional assay (**Figure 4b**).

Furthermore, to corroborate these results, we followed the enzymatic kinetics of nanoalgosomes treated with 1% Triton-X 100 after established time points (*i.e.*, after 1h, 2h, and 3h from the addition of the FDA substrate). As illustrated in Figure 4c, the fluorescence intensity was measured every 15 minutes during this time course test and, as expected, each no-treated sample exhibited a similar trend, namely a linear increase in fluorescence intensity over time. However, this increase ceased upon the addition of 1% Triton-X 100, remaining quite constant until the end of the assay. This trend demonstrates that the fluorescence intensity, corresponding to produced fluorescein, is correlated with membrane integrity of EVs. Indeed, when EVs are lysed the enzymatic reaction halts. Furthermore, the fluorescence values of fluorescein remain quite constant in intact vesicles compared to the respective lysed vesicles over time and for each condition, thereby validating the accurate application of the previously described calibration curve for free fluorescein, which is utilized in calculating nmols of fluorescein produced during the assay.

Based on the results from this section, the optimal conditions for the detectEV assay will involve incubating 2 x 10^{10} EVs with 18 µmol of FDA in a PBS solution, with a final reaction volume of 200 µL, in a 96-well plate. Enzymatic activity, measured through fluorescence emission (excitation at 488 nm, emission at 520 nm), will be followed using a spectrofluorometer for a duration of 3 hours at room temperature. The final readout corresponds to enzymatic units (nmol/min), which will be calculated using a calibration curve of free fluorescein to derive the total nmols produced during the assay. This value will then be divided by the total time (180 minutes) to obtain the final readout in nmol/min.

Application of detectEV assay

Batch-to-batch reproducibility: To assess the detectEV assay's capability in evaluating batch-to-batch reproducibility, we selected four nanoalgosome batches (named Alg1, Alg2, Alg3, Alg4) that exhibited variations in quality during the QC analyses. Following the separation of nanoalgosomes through tangential flow filtration, the application of EV-based QC methods for each production allowed us to identify differences in terms of quality, primarily attributed to the performance or half-life of the TFF cartridges (Paolini et al., 2022; Paterna et al., 2022; Sverdlov, 2012). These differences was revealed by fluorescent-NTA readings, after staining 10^{10} nanoalgosomes with Di-8-ANEPPS, a specific lipophilic fluorescent dye that helps to discriminate between EVs and non-vesicle co-isolates (Adamo et al., 2021). As reported in **figure 5a**, the F-NTA results showed that the selected four batches had a quite similar size distribution, but differences in terms of percentage of Di-8-ANEPPS-positive EVs with respect to the total EVs tracked with NTA in scattering. More specifically, Alg1=10%; Alg2=3%; Alg3=2%, Alg4= unreliable measurement. Subsequently, we applied the detectEV assay for these EV-preparations, using an equal amount of vesicles for all batches (2x10^{10} nanoalgosomes). The results shown in **Figure 5b** identified Alg1 as the one with high enzymatic activity compared to the other three batches analysed. These findings were consistent with the F-NTA results (**Figure 5a**), supporting the proposed functional enzymatic assay as a new single-step method for validating EV preparations and monitoring batch-to-batch variability during EV production.

***Storage conditions*:** The effects of different storage conditions on EVs have been investigated in several studies, demonstrating how various factors related to storage can affect EV characteristics, including membrane stability and EV potency (Sivanantham and Jin, 2022). Recently, more comprehensive studies have systematically compared different storage strategies, to identify appropriate conditions for stabilizing EV preparations, especially for therapeutic applications (Görgens et al., 2022). Following the storage of EV samples, they are usually analysed over time

using various methods, including NTA, bead-based multiplex flow cytometry, and single vesicle imaging flow cytometry (IFCM) (Görgens et al., 2022). Among them, the most commonly used is NTA.

Here, we applied the detectEV assay to monitor the effects of one-week storage under different conditions (including 4°C, -20°C, -80°C, lyophilization in 5% and 8% sucrose) on nanoalgosome bioactivity/stability (**figure 6a)**. In parallel, we performed NTA readings to monitor the size distribution and concentration of nanoalgosomes stored under these conditions. For all the samples analysed, we did not observe changes in size distribution with an average size of 100±20 nm and a quite similar nanoparticle concentration between the samples (**figure 6b, Supporting figure 2**). Conversely, as reported in **figure 6a**, the detectEV assay highlighted a significant and quantifiable reduction of enzymatic activity in EV, less than 1 nmol/min in frozen (-20°C or -80°C) or lyophilized EV-samples, compared to those stored at 4°C for a week. These results demonstrate that the assay can efficiently identify the most appropriate storage method for EV or suggest the EV preparation that could be suitable for future application in specific potency tests (Pachler et al., 2017; Gimona et al., 2021).

***Loading methods*:** Several studies have reported advantages of using EVs as drug delivery systems in preclinical models because of their low toxicity, high targeting capacity, and slow clearance (Gangadaran and Ahn, 2020). Exogenous cargo can be loaded into EVs using various physical methods, including electroporation, sonication, saponin-assisted loading, freeze-thaw cycles, and extrusion (Fu et al., 2020; Jeyaram and Jay, 2017; Kusuma et al., 2018; Lener et al., 2015; Lőrincz et al., 2014; Sokolova et al., 2011). These methods may cause a loss of EV-functionality or damage the integrity of the EV-membrane, even though the phospholipidic bilayer should quickly recover its reclosed integrity after membrane perturbations. In this context, we investigated whether the proposed functional assay could be applied to this type of assessment, testing if it could provide indications of changes or alterations in the biological properties of EVs post-loading (**figure 6c**) (Han et al., 2021; Rankin-Turner et al., 2021). To this end, different loading methods were tested to identify the impact on the integrity and bioactivity of nanoalgosomes (Jamur and Oliver, 2010; Van Deun et al., 2020). For each method, we used the most commonly reported EV loading settings (C. Chen et al., 2021; Herrmann et al., 2021). Contextually, we monitored changes in nanoalgosomes size distribution and concentration after the application of loading method, using NTA (**figure 6d**). In **Figure 6c**, we reported detectEV results, which highlight that freeze and thaw approach appear to be the "gentlest" loading method, with less impact on nanoalgosome features. In contrast, for some conditions used such as electroporation (E1), sonication (S1), saponification (Sap1-2), or extrusion, we observed a

significant decrease in EV-enzymatic activity under 1 nmol/min, probably due to harsh membrane perturbation or loss of vesicle integrity of many vesicles. Interestingly, this difference could not be detected by NTA analysis, as the size (inside the range of 100±20 nm for all samples) and concentration of these samples were similar with the untreated-control (**Figure 6d, Supporting figure 3**). The successful application of the assay for evaluating EVs during loading could be the starting point for developing effective EV-based therapeutics, which might require further investigation in tailoring specific potency assays.

***Comparison between EV-isolation methods*:** EVs derived from different bioresources can be isolated using various approaches. Depending on individual experimental settings (such as small or large-scale production), it is essential to establish the most efficient method for sEV separation while also considering the quality of the EV sample obtained. In Adamo et al. 2021, we demonstrated that different separation procedures (e.g., dUC, TFF, and gUC) allowed us to efficiently isolate nanoalgosomes from microalgal conditioned media. Here, we compared the quality of nanoalgosomes from the same *T. chuii* culture batch, isolated in parallel by dUC and TFF, applying the detectEV assay (Adamo et al., 2021; Picciotto et al., 2021). The results indicated that nanoalgosomes isolated by either method showed the same bioactivity/stability, confirming the good quality of both nanoalgosome preparations (**Figure 7a**).

All these results suggested that by using the proposed functional enzymatic assay, we were able to directly and quantitatively compare EV quality across the two isolation methods, different storage and loading conditions.

detectEV assay to functionally evaluate human EVs

To assess the detectEV assay's applicability to other EVs, we examined its sensitivity, compatibility, and specificity using various EV types, including human EVs isolated from conditioned media. Accordingly, we employed dUC to isolate sEVs from conditioned media of different human cell lines, specifically normal and tumoral mammary epithelial cells, and human embryonic kidney cells (1-7 HB2, MDA MB 231 and HEK 293T cell lines, respectively). As for nanoalgosomes, we first characterized them by evaluating selected MISEV-2023 quality parameters, confirming the right size distribution, morphology and positivity to enriched EV biomarkers (data reported in **Supporting Figure 1**, EV-TRACK ID: EV231004) (Welsh et al., 2024). Following the biochemical and biophysical characterization of these three types of sEVs, we incubated a standardized quantity of sEVs (2 x 10^{10} sEVs) with 18µmol of FDA, according with the detectEV assay setting described before. The results in **figure 7b** confirmed the presence of reliable enzymatic-dependent activity for

all three EV types analyzed, demonstrating detectEV assay's compatibility with human EVs. Interestingly, breast tumor-derived sEVs showed significantly higher enzymatic activity (five-fold increase) compared to sEVs isolated from normal breast cells, opening new perspectives for detectEV assay's application in tumor diagnosis.

detectEV prediction of EV potency

To showcase the predictive capability of the detectEV assay in evaluating the potency of EVs, we performed an antioxidant activity test as a potency assessment, given the robust antioxidant properties of nanoalgosomes (Adamo et al., 2023). We selected nanoalgosome batches with significant differences in quality and bioactivity, as indicated by the detectEV results showed in **Figure 5**. Specifically, we chose Alg1 and Alg3 batches that exhibited significantly higher esterase activity compared to the Alg4 batch.

Subsequently, to establish a customized potency test for nanoalgosomes, 1-7 HB2 cells were exposed to 0.5 μg/mL of Alg1, Alg3, and Alg4 (approximately 10^{10} EVs) to assess their antioxidant bioactivity, particularly in terms of countering reactive oxygen species (ROS) production in cells stressed with the oxidant agent. The results demonstrated that Alg1 and Alg3 effectively mitigated the oxidative stress induced by the oxidant agent, restoring ROS levels near to physiological values, with Alg1 exhibiting strong antioxidant activity (**Figure 8**). In contrast, Alg4 failed to alleviate the stress, indicating no significant antioxidant activity. These outcomes align seamlessly with the detectEV results, highlighting its ability to predict the potency of various EV preparations.

Discussion

The field of extracellular vesicles has made significant advancements; yet determined challenges persist, primarily centred around the lack of reliable functional assays for assessing EV bioactivity (Nguyen et al., 2020). The intricate nature of EV heterogeneity and their regulated mechanisms across different diseases adds complexity to developing robust and universal functional assays. Despite the diversity of available potency assays, challenges in quantitativeness, sensitivity, accuracy, precision, and robustness persist, emphasizing the urgent need for refining and establishing specific test capable of predicting EV potency effectively and for different applications (Pachler et al., 2017; Gimona et al., 2021; Nguyen et al., 2020; Ramirez et al., 2018; Zheng et al., 2023). In this context, this study explores the potential to leverage the presence of cargo enzymes within EVs for the development of a functional enzymatic assay. Specifically, our focus has been on esterase-like enzymes in EVs, as their presence is reported in different proteomic datasets, showing associations with EVs from various

sources (Gonzales et al., 2009; Gonzalez-Begne et al., 2009; Pocsfalvi et al., 2018; Rizzo et al., 2020; Choi et al., 2011; McMillan and Kuehn, 2022). The proposed detectEV assay specifically aims to quantitatively measure esterase activity within EVs, offering a single-step analysis for assessing the bioactivity and quality of EV preparations, using small-sized samples. Notably, this assay does not require washing steps, making it a faster and cost-effective method that offers several advantages, including simplicity. The establishment of the proposed assay involved a meticulous validation of specific parameters (like EV and FDA concentrations, reaction volume, reaction buffer, time, and temperature), ensuring analytical sensitivity and specificity, according to MISEV-2023 (Welsh et al., 2024). Nanoalgosomes, that are microalgal derived-EVs, were employed as EV models in this validation process. While our results demonstrate that the established experimental settings efficiently measure the enzymatic activity of nanoalgosomes, as well as of EVs derived from different mammalian cell lines, these parameters could be further adapted *ad hoc* for EVs from various origins or types, like large EVs or oncosomes. Indeed, different types of EVs could exhibit distinct stability or carry different combinations of esterase-like enzymes as cargo, possibly with high enzymatic activity. Consequently, it might be possible to slightly adapt the assay condition by decreasing the amount of FDA, the time or the vesicle concentration based on specific kinds of EVs, or to establish minimum and maximum ranges of enzymatic activity that qualify whether a vesicle preparation is suitable for subsequent analyses. Therefore, the versatile applicability of the detectEV assay across diverse cellular sources allow for its extension to every EV types with esterase-like activity. This positioning makes it a potentially universal measure of EV functionality. The strong innovation introduced by the detectEV assay is its ability to simultaneously measure both the bioactivity and membrane integrity of vesicles. Specifically, our results illustrated that when the vesicle integrity is perturbed and/or completely lost, the enzymatic activity decrease or becomes undetectable by the detectEV assay. This observation could be attributed to several reasons. First of all, there could be a potential reduction in the enzymatic activity of esterases when released into the extra-vesicular environment, as compared to the optimal condition of the vesicular lumen. Accordingly, when analysing the results of the detectEV assay described for nanoalgosomes subjected to different loading methods (such as sonication or electroporation), *i.e.*, physical methods that slightly perturb vesicular membrane without compromising its complete integrity, the assay is capable of detecting enzymatic activity, albeit to a lesser extent. This suggests that the proposed assay can provide a value that closely correlates the bioactivity and the quality of the vesicles, as well as the integrity of their membrane. Another relevant aspect to consider is the detectEV assay's applicability, like its ability to highlight batch-to-batch variation between EV preparations. Indeed, the detectEV results were in

complete agreement with the F-NTA data obtained from diverse nanoalgosome batches, showing that purer vesicles (Alg1) had also higher enzymatic activity. Additionally, Alg1 has been shown to be the nanoalgosome preparation that most efficiently counterbalances cell-oxidative stress *in vitro*, as observed in a specific potency test for nanoalgosomes (antioxidant activity assay). This suggests that the detectEV result could predict which vesicle preparation possesses greater specific potency for subsequent preclinical or clinical analyses. Further, other practical applications demonstrate its effectiveness in reproducibility assessments, highlighting changes in EV functionality under different conditions (i.e., different storage methods) and comparing the quality of EVs after various isolation techniques, adhering to all the guidelines outlined in the MISEV-2023 for the development of specific functional assays for extracellular vesicles (Welsh et al., 2024)In conclusion, the detectEV assay extend labelling approaches for EVs using FDA-like molecules (e.g., Calcein-AM, CFSE, or others) already employed for flow cytometry analysis or exploiting other specific substrates for enzymes present in EV cargo (Ender et al., 2020; Nikiforova et al., 2021; Tertel et al., 2022; Kormelink et al., 2016). The assay's flexibility could also be extended to diagnostic applications, exploring its capacity to discern pathological conditions, like tumour, based on EV bioactivity in samples derived from liquid biopsies (like plasma and urine), aligning with the growing importance of EVs as theranostics (Liang et al., 2021). To conclude, we propose that alongside efforts to harmonize EV nomenclature and characterization, the detectEV assay could represent a solution to existing challenges in functional assays for EVs.

Materials and Methods

Nanoalgosomes and cell derived-EVs are isolated and characterized as previously described in Adamo G. et al., 2021, and the relative methods are reported in Supporting methods.

Set up of functional enzymatic assay: pilot test. Fluorescein diacetate (FDA, Sigma-Aldrich) stock solution was prepared in acetone at a final concentration of 2 mg/mL. 2 x 10^{10} nanoalgosomes were incubated with 35 µmol of FDA, reaching a final volume of 200 µl with 0.2 µm filtered PBS without Ca^{++} and Mg^{++}. The same amount of FDA was added to 0.2 µm filtered PBS without Ca^{++} and Mg^{++} (nanoalgosome-vehicle). Fluorescence emission was measured every 15 minutes, up to 16 h, using a blue filter of the GloMax Discover Microplate Reader.

Preparation fluorescein standards curve. Fluorescein sodium salt (ex/em 490/514 nm, Sigma-Aldrich) was used to generate a standard calibration curve.
The fluorescence intensity of serial dilutions of fluorescein (from 300 nmol to 0 nmol), diluted in PBS without Ca^{++} and Mg^{++} at a final volume of 200 µl, was measured in a 96-well-plate using a blue filter of the GloMax Discover Microplate Reader (Promega).

Measure of enzymatic activity. To calculate the specific enzymatic activity, the enzyme units (U), the amount of esterases that catalyses the reaction of 1 nmol of substrate into product per minute, was determined. EV enzymatic activity values were expressed in U as nanomoles of fluorescein produced per minute (nmol/min). This value was determined by fitting the fluorescence intensities measured at the end of the functional assay to the fluorescein concentration of the standard curve. Subsequently, this value was divided by the total assay time (180 minutes) to obtain the nanomoles per minute.

Michaelis–Menten Kinetic. 2 x 10^{10} nanoalgosmes were incubated with different concentrations of FDA (0, 1.6, 3.3, 6.6, 13, 26 x 10^3 nmol) dissolved in 0.2 µm filtered PBS without Ca^{++} and Mg^{++}, in a final volume equal to 200 µl. The fluorescence emission was followed until 3 hours, in a 96-well-plate using a blue filter of the GloMax Discover Microplate Reader (Promega). Obtained values were corrected by subtracting background fluorescence value (i.e., PBS with FDA). Fitting these data to the standard calibration curve, the Michaelis–Menten equation was applied using nonlinear regression and plotting the reaction's initial rates (nmol/min) as a function of FDA concentration. Vmax and Km were found using GraphPad software.

Analytical sensitivity. Serial dilutions of nanoalgosomes (from 2 x 10^{10} to 3 × 10^8 sEVs) were incubated with 18 µmol of FDA, reaching a final volume of 200 µl with 0.2 µm filtered PBS without

Ca^{++} and Mg^{++}. Fluorescence emission was followed up to 3h, using a blue filter of the GloMax Discover Microplate Reader. The same amount of FDA was added to 0.2 µm-filtered PBS without Ca^{++} and Mg^{++} (nanoalgosome-vehicle). This background fluorescence value was subtracted from the fluorescence intensity values of each sample, for all the condition described.

Analytical specificity. 2 x 10^{10} nanoalgosomes were incubated with 0.1, 0.25, 0.5 and 1% Triton-X100 (Sigma-Aldrich) for 30 min at room temperature. The same amount of nanoalgosomes were boiled at 100°C for 10 min. Next, samples were incubated with 18 µmol of FDA, reaching a final volume of 200 µl with 0.2 µm filtered PBS without Ca^{++} and Mg^{++}. Fluorescence emission was followed up to 3h, and enzymatic activity was determined as described previously. As control, the same amount of FDA was added to 0.2 µm-filtered PBS without Ca^{++} and Mg^{++} boiled at 100°C for 10 min or with 0.1, 0.25, 0.5 and 1% Triton-X 100. This background fluorescence value was subtracted from the fluorescence intensity values of each respective sample.
Additionally, 2 x 10^{10} nanoalgosomes were incubated with 18 µmol of FDA, reaching a final volume of 200 µl with 0.2 µm filtered PBS without Ca^{++} and Mg^{++}. During the time course of the detectEV assay, specifically after 1, 2, and 3 hours post FDA addition, nanoalgosomes were treated with 1% Triton-X 100. Fluorescence emission was measured every 15 minutes, up to 195 minutes, using a blue filter of the GloMax Discover Microplate Reader. As control, the same amount of FDA was added to 0.2 µm-filtered PBS with/without Ca^{++} and Mg^{++} with 1% Triton X-100. This background fluorescence value was subtracted from the fluorescence intensity values of each respective sample.

Application of detectEV assay

Batch-to-batch reproducibility. 2 x 10^{10} nanoalgosomes from different batches (named Alg1, Alg2, Alg3 and Alg4) were incubated with 18 µmol of FDA, reaching a final volume of 200 µl with 0.2 µm filtered PBS without Ca^{++} and Mg^{++}. Fluorescence emission was followed up to 3h, and enzymatic activity was determined as described above. As negative controls, nanoalgosomes were boiled at 100°C for 10 min.

Storage conditions. Nanoalgosomes were stored for 10 days at different condition: 4°C, -20°C, −80 °C and upon lyophilization in 5% and 8% sucrose, at 4°C for a week. Lyophilized samples were carefully rehydrated in 0.2 µm-filtered Milli-Q water. After NTA analysis on all stored samples, detectEV assay was performed, as described previously.

Loading methods. 2 x 10^{12} nanoalgosomes (and nanoalgosome-vehicle, *i.e.* 0.2 µm filtered PBS without Ca^{++} and Mg^{++}, used as a negative control) underwent the subsequent treatments:
-Electroporation was performed in Gene Pulser cuvettes (0.4 cm cell electrode gap) on a BioRad Gene Pulser equipped with a capacitance extender, with two conditions selected, E1 (125 µF, 400 V and 2 pulse time of 20 ms) and E2 (125 µF, 250 V and 2 pulse time of 30 ms). -Sonication was performed using two settings: ultrasonic probe sonicator (S1) with 20% amplitude for six cycles of 30 seconds on/off for a total of 3 min, with 2 min cooling, then incubation for 60 min at 37°C; ultrasonic bath (S2) 40 KHz, 40% amplitude for 2 cycles of 30 seconds on/off, then incubation for 60 min at 37°C.
-Freeze–Thaw was performed in 3 cycles of freezing at -80° for 30 min and thawing at room temperature (RT) for 30 min.
-Saponin treatment was performed using two settings: incubation with 0.1 mg/mL (Sap1) and 0.002 mg/mL (Sap2) of saponin (Sigma-Aldrich) at RT for 10 min.
-Extrusion using a mini-extruder equipped with polycarbonate membrane filters of 100 nm and 200 nm pore size (Avestin, Manheim, Germany). Each sample was extruded 31 times.
After the application of each method, NTA analysis was performed on all samples. Next, the enzymatic functional assay was performed, as described previously.

Isolation methods. 2 x 10^{10} nanoalgosomes of the same *T. chuii* conditioned media, isolated by dUC and TFF, were used to perform the functional enzymatic assay, using the same settings described before.

detectEV assay in human-derived sEVs. 2x10^{10} sEVs isolated from MDA MB231, 1-7 HB2, and HEK 293T cells were employed to conduct the detectEV assay, using the same experimental setting described for nanoalgosomes.

Antioxidant activity assay

Intracellular ROS levels in living cells were assessed by employing 2′, 7′-dichlorofluorescein diacetate (DCF-DA; Sigma-Aldrich). DCF-DA undergoes oxidation to form fluorescent DCF (2′, 7′-dichlorofluorescein) in the presence of reactive oxygen species (ROS), enabling detection using a spectrofluorometer. The antioxidant assay was conducted on 1-7 HB2 cell line. Specifically, 4x10^3 cells were plated in 96-well microplates for 24 hours. Subsequently, cells were treated with Alg1, Alg3 and Alg4 (0.5 µg/mL, 10^{10} EVs/mL) for an additional 24 hours. Following removal of the medium, cells were exposed to PBS containing 40 µM of DCF-DA and incubated in a humidified atmosphere (5% CO2 at 37°C) for 1 hour. The cells were then subjected to treatment with or without

the oxidative agents TBH (250 μM for 1 hour) (tert-butyl hydroperoxide solution, Sigma-Aldrich), in the absence or presence of nanoalgosomes. Untreated cells served as a control to establish the baseline intracellular ROS percentage. After thorough washing steps, fluorescence intensity was measured using a fluorescence plate reader with an excitation wavelength of 485 nm and an emission wavelength of 538 nm (GloMax® Discover Microplate Reader, Promega). The relative percentage of intracellular ROS was normalized respect to untreated cells (control).

Statistical analysis

Each measurement reported here was repeated as experimental triplicate, and mean values, as well as standard deviations, were calculated. One-way ANOVA analysis was performed using GraphPad software.

Author Contributions (CRediT)

Giorgia Adamo: Conceptualization, Investigation, Methodology, Formal analysis, Visualization, Validation, Funding acquisition, Writing - Original Draft and Final Review & Editing; **Sabrina Picciotto:** Methodology, Formal analysis, Data curation, Software, Writing - Original Draft; **Paola Gargano:** Formal analysis, Data curation, Software, Writing - Original Draft; **Angela Paterna**: Formal analysis, Data curation; **Samuele Raccosta**: Formal analysis, Data curation; **Estella Rao**: Formal analysis, Data curation; **Daniele Paolo Romancino**: Formal analysis, Data curation, **Giulio Ghersi:** Data curation, Final Review; **Mauro Manno**: Formal analysis, Data curation; Final Review; **Monica Salamone:** Formal analysis, Data curation; **Antonella Bongiovanni**: Conceptualization, Investigation, Validation, Writing - Original Draft and Review & Editing, Supervision, Visualization, Project administration, Funding acquisition; Final Review & Editing.

Conflicts of interest

The authors declare the following financial competing interests: AB, MM, and NT have filed the patent (PCT/EP2020/086622) related to microalgal-derived extracellular vesicles described in the paper. GA, SP, and AB have filed the patent (PCT/IB2024/052194) related to the detectEV assay.. The remaining authors declare no competing interests.

Associated Content

Supporting information (PDF) contains additional figures and detailed supplementary methods; this file is available free of charge.

Funding Sources

This work was supported by the VES4US and the BOW projects, funded by the European Union's Horizon 2020 research and innovation programme, under grant agreements nos. 801338 and 952183, and by the Institute for Research and Biomedical Innovation (IRIB), National Research Council of Italy (CNR) of Palermo (Internal Call@IRIB2023).

Notes and references

Adam G, Duncan H: Development of a sensitive and rapid method for the measurement of total microbial activity using fluorescein diacetate (FDA) in a range of soils. Soil Biology and Biochemistry 2001; 33: 943–951.

Adamo G, Santonicola P, Picciotto S, et al: Harnessing Nature's NanoSecrets: Biocompatibility, Biodistribution and Bioactivity of Extracellular Vesicles Derived from Microalgae. bioRxiv 2023; 04.04.535547.

Adamo G, Fierli D, Romancino DP et al.: Nanoalgosomes: Introducing extracellular vesicles produced by microalgae. Journal of Extracellular Vesicles 2021; 10: e12081.

Bisswanger H: Enzyme assays. Perspectives in Science 2014; 1: 41–55.

Bleackley MR, Samuel M, Garcia-Ceron D et al.: Extracellular Vesicles From the Cotton Pathogen Fusarium oxysporum f. sp. vasinfectum Induce a Phytotoxic Response in Plants. Frontiers in Plant Science 2020; 10.

Bruno S, Tapparo M, Collino F et al.: Renal Regenerative Potential of Different Extracellular Vesicle Populations Derived from Bone Marrow Mesenchymal Stromal Cells. Tissue Eng Part A 2017; 23: 1262–1273.

Chen C, Sun M, Wang J, Su L, Lin J, Yan X: Active cargo loading into extracellular vesicles: Highlights the heterogeneous encapsulation behaviour. Journal of Extracellular Vesicles 2021; 10: e12163.

Chen Y, Zhao Y, Yin Y, Jia X, Mao L: Mechanism of cargo sorting into small extracellular vesicles. Bioengineered 2021; 12: 8186–8201.

Choi B, Rempala GA, Kim JK: Beyond the Michaelis-Menten equation: Accurate and efficient estimation of enzyme kinetic parameters. Sci Rep 2017; 7: 17018.

Choi D-S, Kim D-K, Choi SJ et al.: Proteomic analysis of outer membrane vesicles derived from Pseudomonas aeruginosa. Proteomics 2011; 11: 3424–3429.

Cygler M, Schrag JD, Sussman JL, et al.: Relationship between sequence conservation and three-dimensional structure in a large family of esterases, lipases, and related proteins. Protein Science 1993; 2(3):366-382.

Duggleby RG: Experimental designs for estimating the kinetic parameters for enzyme-catalysed reactions. J Theor Biol 1979; 81: 671–684.

Duggleby RG, Wood C: Analysis of progress curves for enzyme-catalysed reactions. Automatic construction of computer programs for fitting integrated rate equations. Biochem J 1989; 258: 397–402.

Dzionek A, Dzik J, Wojcieszyńska D, Guzik U: Fluorescein Diacetate Hydrolysis Using the Whole Biofilm as a Sensitive Tool to Evaluate the Physiological State of Immobilized Bacterial Cells. Catalysts 2018; 8: 434.

Ender F, Zamzow P, von Bubnoff N, Gieseler F: Detection and Quantification of Extracellular Vesicles via FACS: Membrane Labeling Matters! International Journal of Molecular Sciences 2020; 21: 291.

Fontvieille DA, Outaguerouine A, Thevenot DR: Fluorescein diacetate hydrolysis as a measure of microbial

activity in aquatic systems: Application to activated sludges. Environmental Technology 1992; 13: 531–540.

Fu S, Wang Y, Xia X, Zheng JC: Exosome engineering: Current progress in cargo loading and targeted delivery. NanoImpact 2020; 20: 100261.

Gangadaran P, Ahn B-C: Extracellular Vesicle- and Extracellular Vesicle Mimetics-Based Drug Delivery Systems: New Perspectives, Challenges, and Clinical Developments. Pharmaceutics 2020; 12: 442.

Garcia-Ceron D, Lowe RGT, McKenna JA et al.: Extracellular Vesicles from Fusarium graminearum Contain Protein Effectors Expressed during Infection of Corn. Journal of Fungi 2021; 7: 977.

Gimona M, Brizzi MF, Choo ABH et al.: Critical considerations for the development of potency tests for therapeutic applications of mesenchymal stromal cell-derived small extracellular vesicles. Cytotherapy 2021; 23: 373–380.

Gonzales PA, Pisitkun T, Hoffert JD et al.: Large-scale proteomics and phosphoproteomics of urinary exosomes. J Am Soc Nephrol 2009; 20: 363–379.

Gonzalez-Begne M, Lu B, Han X et al.: Proteomic analysis of human parotid gland exosomes by multidimensional protein identification technology (MudPIT). J Proteome Res 2009a; 8: 1304–1314.

Görgens A, Corso G, Hagey DW et al.: Identification of storage conditions stabilizing extracellular vesicles preparations. Journal of Extracellular Vesicles 2022; 11: e12238.

Gray WD, Mitchell AJ, Searles CD: An accurate, precise method for general labeling of extracellular vesicles. MethodsX 2015; 2: 360–367.

Guidance for Industry Potency Tests for Cellular and Gene Therapy Products: n.d.

Han Y, Jones TW, Dutta S et al.: Overview and Update on Methods for Cargo Loading into Extracellular Vesicles. Processes 2021; 9: 356.

Herrmann IK, Wood MJA, Fuhrmann G: Extracellular vesicles as a next-generation drug delivery platform. Nat Nanotechnol 2021; 16: 748–759.

Hutter JL, Bechhoefer J: Calibration of atomic-force microscope tips. Review of Scientific Instruments 1993; 64: 1868–1873.

Jamur MC, Oliver C: Permeabilization of cell membranes. Methods Mol Biol 2010; 588: 63–66.

Jeyaram A, Jay SM: Preservation and Storage Stability of Extracellular Vesicles for Therapeutic Applications. AAPS J 2017; 20: 1.

Kormelink TG, Arkesteijn GJA, Nauwelaers FA, van den Engh G, Nolte-’t Hoen ENM, Wauben MHM: Prerequisites for the analysis and sorting of extracellular vesicle subpopulations by high-resolution flow cytometry. Cytometry Part A 2016; 89: 135–147.

Kusuma GD, Barabadi M, Tan JL, Morton DAV, Frith JE, Lim R: To Protect and to Preserve: Novel Preservation Strategies for Extracellular Vesicles. Frontiers in Pharmacology 2018; 9.

Lener T, Gimona M, Aigner L et al.: Applying extracellular vesicles based therapeutics in clinical trials - an ISEV position paper. J Extracell Vesicles 2015; 4: 30087.

Liang Y, Lehrich BM, Zheng S, Lu M: Emerging methods in biomarker identification for extracellular vesicle-based liquid biopsy. Journal of Extracellular Vesicles 2021; 10: e12090.

Lőrincz ÁM, Timár CI, Marosvári KA et al.: Effect of storage on physical and functional properties of extracellular vesicles derived from neutrophilic granulocytes. J Extracell Vesicles 2014; 3: 10.3402/jev.v3.25465.

McMillan HM, Kuehn MJ: Proteomic Profiling Reveals Distinct Bacterial Extracellular Vesicle Subpopulations with Possibly Unique Functionality. Applied and Environmental Microbiology 2022; 89: e01686-22.

Michaelis L, Menten ML, Johnson KA, Goody RS: The original Michaelis constant: translation of the 1913 Michaelis-Menten paper. Biochemistry 2011; 50: 8264–8269.

Morales-Kastresana A, Telford B, Musich TA et al.: Labeling Extracellular Vesicles for Nanoscale Flow Cytometry. Sci Rep 2017; 7: 1878.

Nguyen VVT, Witwer KW, Verhaar MC, Strunk D, van Balkom BWM: Functional assays to assess the therapeutic potential of extracellular vesicles. J Extracell Vesicles 2020; 10: e12033.

Nikiforova N, Chumachenko M, Nazarova I et al.: CM-Dil Staining and SEC of Plasma as an Approach to Increase Sensitivity of Extracellular Nanovesicles Quantification by Bead-Assisted Flow Cytometry. Membranes 2021; 11.

O'Grady T, Njock M-S, Lion M et al.: Sorting and packaging of RNA into extracellular vesicles shape intracellular transcript levels. BMC Biology 2022; 20: 72.

Pachler K, Ketterl N, Desgeorges A et al.: An In Vitro Potency Assay for Monitoring the Immunomodulatory Potential of Stromal Cell-Derived Extracellular Vesicles. Int J Mol Sci 2017; 18: 1413.

Paolini L, Monguió-Tortajada M, Costa M et al.: Large-scale production of extracellular vesicles: Report on the "massivEVs" ISEV workshop. Journal of Extracellular Biology 2022; 1: e63.

Paterna A, Rao E, Adamo G et al.: Isolation of Extracellular Vesicles From Microalgae: A Renewable and Scalable Bioprocess. Front Bioeng Biotechnol 2022; 10: 836747.

Perna RF, Tiosso PC, Sgobi LM et al.: Effects of Triton X-100 and PEG on the Catalytic Properties and Thermal Stability of Lipase from Candida Rugosa Free and Immobilized on Glyoxyl-Agarose. Open Biochem J 2017; 11:66-76.

Picciotto S, Barone ME, Fierli D et al.: Isolation of extracellular vesicles from microalgae: towards the production of sustainable and natural nanocarriers of bioactive compounds. Biomater Sci 2021; 9: 2917–2930.

Picciotto S, Santonicola P, Paterna A et al.: Extracellular Vesicles From Microalgae: Uptake Studies in Human Cells and Caenorhabditis elegans. Front Bioeng Biotechnol 2022; 10: 830189.

Pocsfalvi G, Turiák L, Ambrosone A et al.: Protein biocargo of citrus fruit-derived vesicles reveals heterogeneous transport and extracellular vesicle populations. J Plant Physiol 2018; 229: 111–121.

Pospichalova V, Svoboda J, Dave Z et al.: Simplified protocol for flow cytometry analysis of fluorescently

labeled exosomes and microvesicles using dedicated flow cytometer. Journal of Extracellular Vesicles 2015; 4: 25530.

Raposo G, Stoorvogel W: Extracellular vesicles: exosomes, microvesicles, and friends. Journal of Cell Biology 2013; 200(4):373-83.Ramirez MI, Amorim MG, Gadelha C et al.: Technical challenges of working with extracellular vesicles. Nanoscale 2018; 10: 881–906.

Rankin-Turner S, Vader P, O'Driscoll L, Giebel B, Heaney LM, Davies OG: A call for the standardised reporting of factors affecting the exogenous loading of extracellular vesicles with therapeutic cargos. Advanced Drug Delivery Reviews 2021; 173: 479–491.

Rizzo J, Chaze T, Miranda K et al.: Characterization of Extracellular Vesicles Produced by Aspergillus fumigatus Protoplasts. mSphere 2020; 5: e00476-20.

Robinson PK: Enzymes: principles and biotechnological applications. Essays Biochem 2015; 59: 1–41.

de Rond L, van der Pol E, Hau CM et al.: Comparison of Generic Fluorescent Markers for Detection of Extracellular Vesicles by Flow Cytometry. Clinical Chemistry 2018; 64: 680–689.

Simpson RJ, Kalra H, Mathivanan S: ExoCarta as a resource for exosomal research. Journal of Extracellular Vesicles 2012; 1: 18374.

Sivanantham A, Jin Y: Impact of Storage Conditions on EV Integrity/Surface Markers and Cargos. Life 2022; 12: 697.

Sırt Çıplak E, Akoğlu KG: Enzymatic Activity as a Measure of Total Microbial Activity on Historical Stone. Heritage 2020; 3: 671–681.

Sokolova V, Ludwig A-K, Hornung S et al.: Characterisation of exosomes derived from human cells by nanoparticle tracking analysis and scanning electron microscopy. Colloids Surf B Biointerfaces 2011; 87: 146–150.

Sun Y, Liu G, Zhang K, Cao Q, Liu T, Li J: Mesenchymal stem cells-derived exosomes for drug delivery. Stem Cell Res Ther 2021; 12: 561.

Sverdlov ED: Amedeo Avogadro's cry: What is 1 μg of exosomes? BioEssays 2012; 34: 873–875.

Tertel T, Schoppet M, Stambouli O, Al-Jipouri A, James PF, Giebel B: Imaging flow cytometry challenges the usefulness of classically used extracellular vesicle labeling dyes and qualifies the novel dye Exoria for the labeling of mesenchymal stromal cell–extracellular vesicle preparations. Cytotherapy 2022; 24: 619–628.

US FDA. Guidance for industry on potency tests for cellular and gene therapy products 2011. Available at: https://www.fda.gov/regulatory-information/search-fda-guidance-documents/potency-tests-cellular-and-gene-therapy-products

Van Deun J. et al.: EV-TRACK: transparent reporting and centralizing knowledge in extracellular vesicle research. Nat Methods. 2017; 14: 228-232.

Van Deun J, Roux Q, Deville S et al.: Feasibility of Mechanical Extrusion to Coat Nanoparticles with Extracellular Vesicle Membranes. Cells 2020; 9: 1797.

Welsh JA, Goberdhan DCI, O'Driscoll L, et al: Minimal information for studies of extracellular vesicles

(Misev2023): From basic to advanced approaches. J of Extracellular Vesicle. 2024;13(2):e12404.

Yáñez-Mó M, Siljander PR, Andreu Z et al.:Biological properties of extracellular vesicles and their physiological functions. Journal of extracellular vesicles 2015; 4(1):27066.

Yekula A, Muralidharan K, Kang KM, Wang L, Balaj L, Carter BS: From laboratory to clinic: Translation of extracellular vesicle based cancer biomarkers. Methods 2020; 177: 58–66.

Zheng D, Ruan H, Chen W et al.: Advances in extracellular vesicle functionalization strategies for tissue regeneration. Bioactive Materials 2023; 25: 500–526.

Manuscript Figures

DetectEV: a functional enzymatic assays to predict the potency of extracellular vesicles

Giorgia Adamo,[*a] Sabrina Picciotto,[a] Paola Gargano,[a] Angela Paterna,[b] Samuele Raccosta,[b] Estella Rao,[b] Daniele Paolo Romancino,[a] Giulio Ghersi,[c] Mauro Manno,[b] Monica Salamone [a], and Antonella Bongiovanni.[*a]

a. Cell-Tech HUB and Institute for Research and Biomedical Innovation (IRIB), National Research Council of Italy (CNR), Palermo 90146, Italy.

b. Cell-Tech HUB and Institute of Biophysics (IBF) - CNR, Via Ugo La Malfa 153, 90146 Palermo, Italy.

c. Department of Biological, Chemical and Pharmaceutical Sciences and Technologies (STEBICEF), University of Palermo, 90128 Palermo, Italy.

Giorgia Adamo and Sabrina Picciotto contributed equally to this work.

Corresponding Authors: *giorgia.adamo@irib.cnr.it; *antonella.bongiovanni@irib.cnr.it.

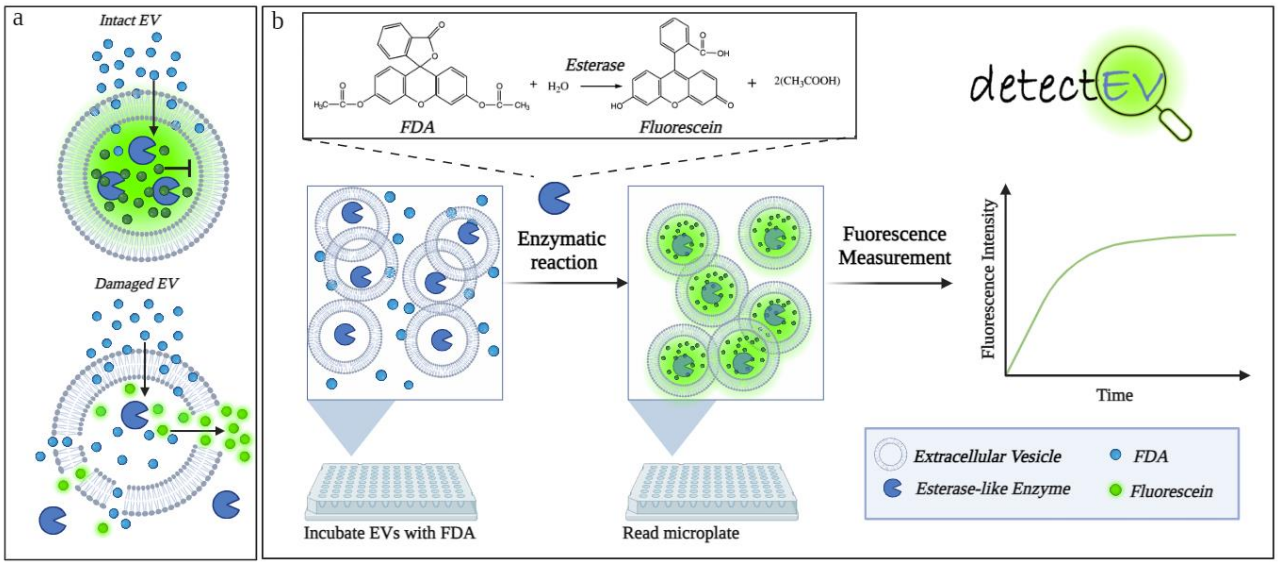

Figure 1. a) Graphic representation of FDA behaviour in intact and damaged EV. b)Schematic representation of the strategy applied for the development of the detectEV assay for extracellular vesicles. Created with BioRender.com.

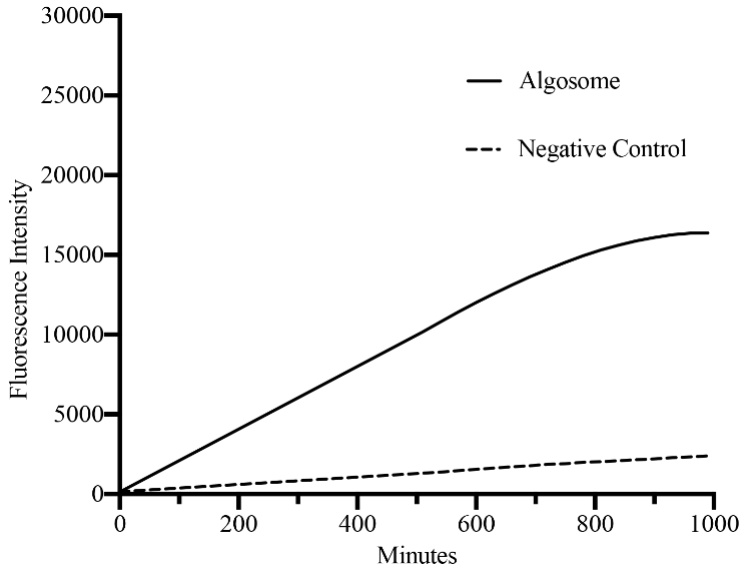

Figure 2. Graph of time-dependent increase of fluorescence intensity of representative microalgal-derived extracellular vesicles (*i.e.* nanoalgosomes) incubated with FDA, compared to a negative control (*i.e.* PBS, vehicle control).

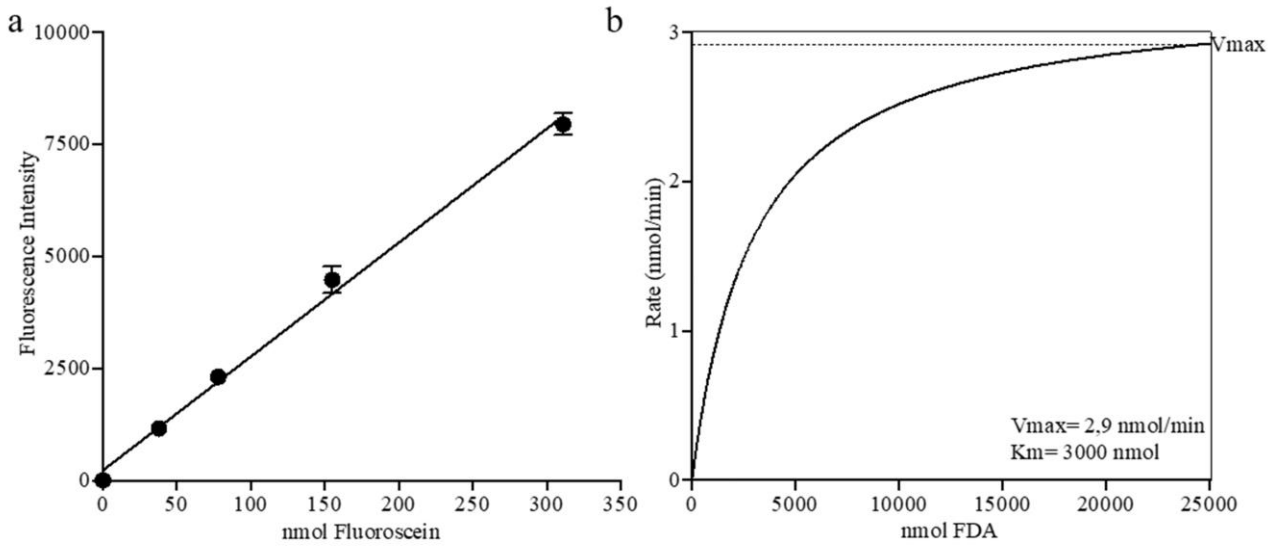

Figure 3. a) Calibration curve of fluorescein. b) Michaelis-Menten graph for the enzymatic cleavage of FDA catalysed by nanoalgosome enzymes.

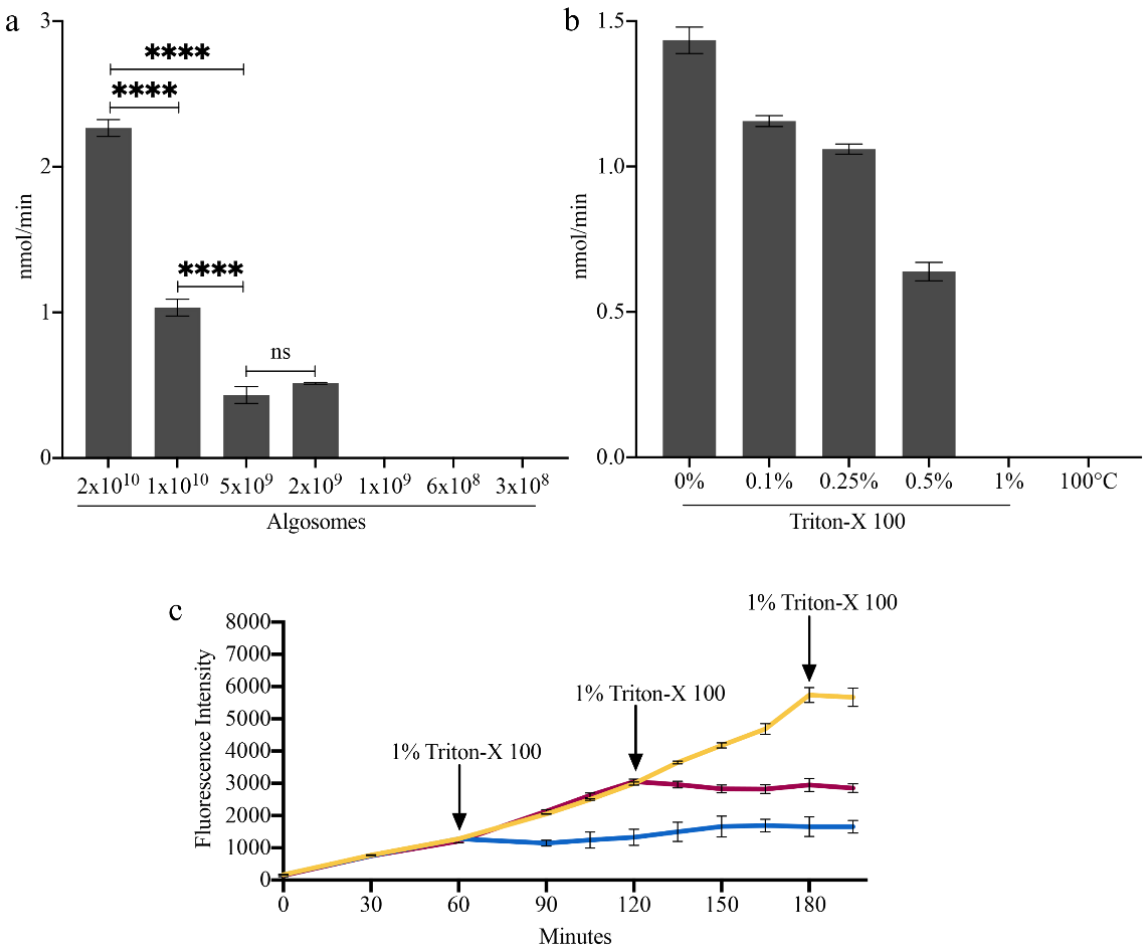

Figure 4. Set up of detectEV enzymatic assay on nanoalgosomes using: a) different concentrations of nanoalgosomes (from 2 x 10^{10} to 3 x 10^{8} sEVs) for detection limit determination (One-way ANOVA was used to assess the statistical significance of the differences: ****$p < 0.0001$, ns=not significant); b) nanoalgosomes untreated and treated with detergent (0.1, 0.25, 0.5, 1% Triton-X 100) and boiled at 100°C (One-way ANOVA was used to assess the statistical significance of the differences: for nanoalgosomes 0% vs nanoalgosomes treated with Triton-X 100 at 0.1, 0.25, 0.5, 1% and vs nanoalgosomes at 100°C, ****$p < 0.0001$ for all conditions). c) Fluorescence intensity measurements of nanoalgosomes treated with 1% Triton-X 100 after 1h, 2h, and 3h from the addition of the FDA substrate.

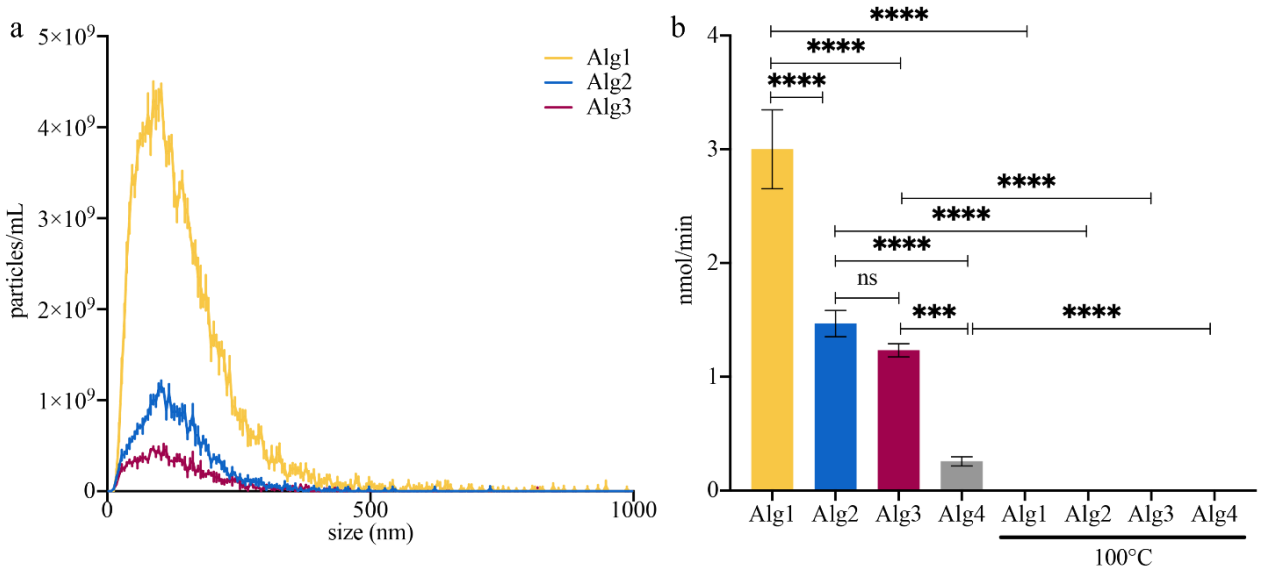

Figure 5. Comparison between different nanoalgosome batches: a) F-NTA and b) detectEV assay on different nanoalgosome batches (Alg1, Alg2, Alg3, Alg4). F-NTA measurement for Alg4 was unreliable. (One-way ANOVA was used to assess the statistical significance of the differences: ****$p < 0.0001$).

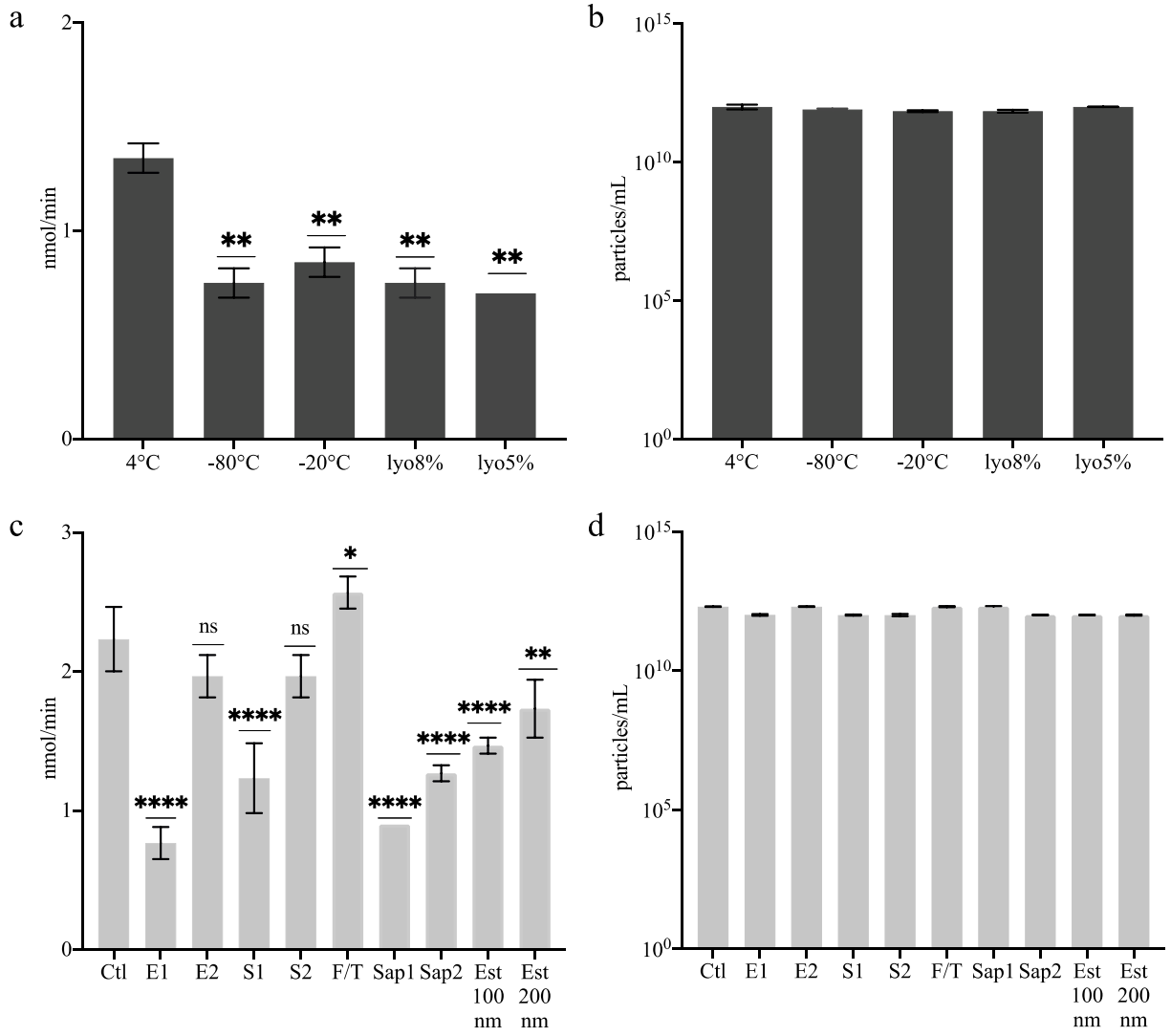

Figure 6. Effect of different storage conditions on nanoalgosomes analyzed by a) detectEV assay (nmol/min) and by b) NTA (particles/mL); (One-way ANOVA was used to assess the statistical significance of the differences 4°C vs -80°C, -20°C, lyo8%, lyo5%; **$p < 0.01$; no significant differences were observed in the NTA data). Effect of different loading methods on nanoalgosomes analyzed by c) detectEV assay (nmol/min) and b) NTA (particles/mL). One-way ANOVA was used to assess the statistical significance of the differences: Ctl vs (E1, S1, Sap.1, Sap.2 Est100nm), ****$p < 0.0001$; Ctl vs (E2, S2), ns=not significant; Ctl vs F/T, *$p < 0.05$; Ctl vs Est200nm, **$p < 0.01$; no significant differences were observed in the NTA data.

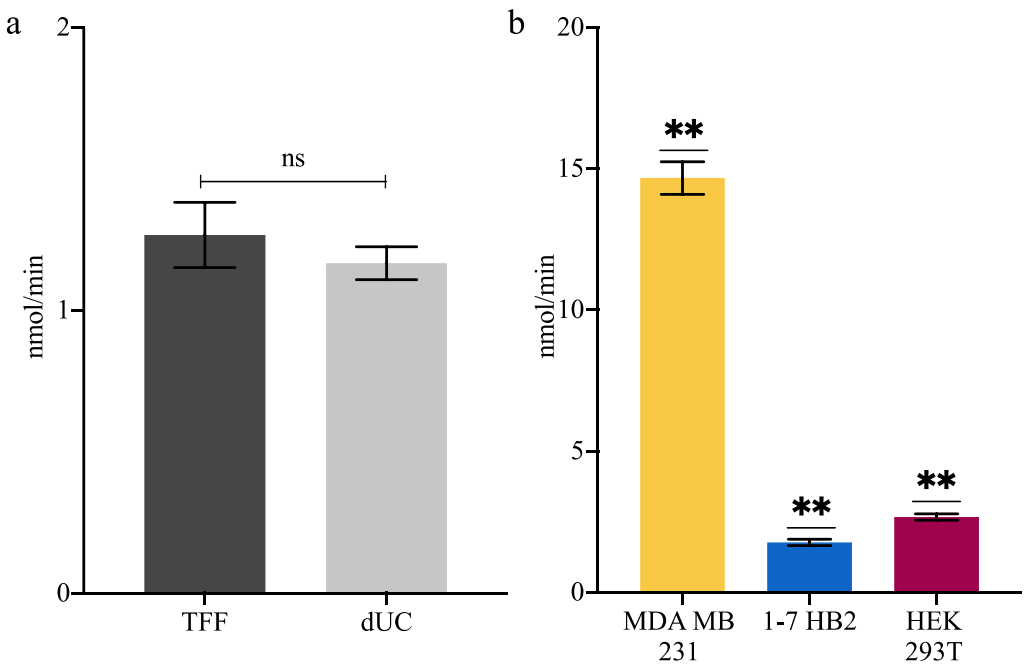

Figure 7. Application of detectEV assay on nanoalgosomes after different a) isolation methods and b) on sEVs from human cell lines (MDA MB 231, 1-7 HB2, HEK 293T cell lines). One-way ANOVA was used to assess the statistical significance of the differences: TFF vs dUC, ns=not significant; MDA MB 231 vs 1-7 HB2, ***$p < 0.001$; MDA MB 231 vs HEK 293T, ***$p < 0.001$; 1-7 HB2 vs HEK 293T, *$p<0.05$.

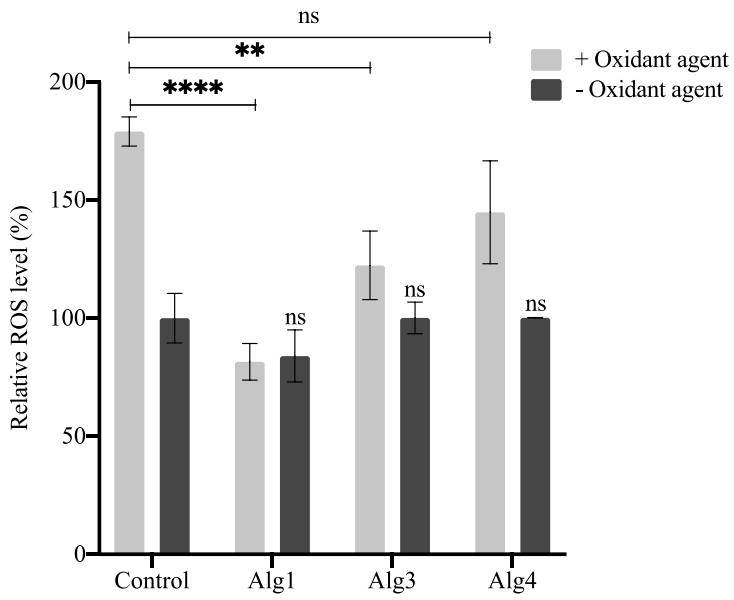

Figure 8. Antioxidant activity of different nanoalgosome batches in 1-7 HB2 cells. ROS production in 1-7 HB2 cells treated with 0.5 µg/mL nanoalgosome for 24h, with/without oxidant agent (250 µM TBH), normalized to negative control (untreated cells). Values are means ± standard deviation of three independent experiments. One-way ANOVA was used to assess the statistical significance of the differences: 1-7 HB2 (- Oxidant agent) vs 1-7 HB2 treated with Alg1, Alg3, Alg4 (- Oxidant agent), ns=not significant; 1-7 HB2 (+ Oxidant agent) vs 1-7 HB2 treated with Alg1 (+ Oxidant agent), ****$p<0.0001$; 1-7 HB2 (+ Oxidant agent) vs 1-7 HB2 treated with Alg3 (+ Oxidant agent); **$p<0.01$; 1-7 HB2 (+ Oxidant agent) vs 1-7 HB2 treated with Alg4 (+ Oxidant agent), ns=not significant.

-Supporting Information-

DetectEV: a functional enzymatic assays to predict the potency of extracellular vesicles

Giorgia Adamo,[*a] Sabrina Picciotto,[a] Paola Gargano,[a] Angela Paterna,[b] Samuele Raccosta,[b] Estella Rao,[b] Daniele Paolo Romancino,[a] Giulio Ghersi,[c] Mauro Manno,[b] Monica Salamone [a], and Antonella Bongiovanni.[*a]

a. Cell-Tech HUB and Institute for Research and Biomedical Innovation (IRIB), National Research Council of Italy (CNR), Palermo 90146, Italy.

b. Cell-Tech HUB and Institute of Biophysics (IBF) - CNR, Via Ugo La Malfa 153, 90146 Palermo, Italy.

c. Department of Biological, Chemical and Pharmaceutical Sciences and Technologies (STEBICEF), University of Palermo, 90128 Palermo, Italy.

Giorgia Adamo and Sabrina Picciotto contributed equally to this work.

Corresponding Authors: *giorgia.adamo@irib.cnr.it; *antonella.bongiovanni@irib.cnr.it.

- Supporting Figures -

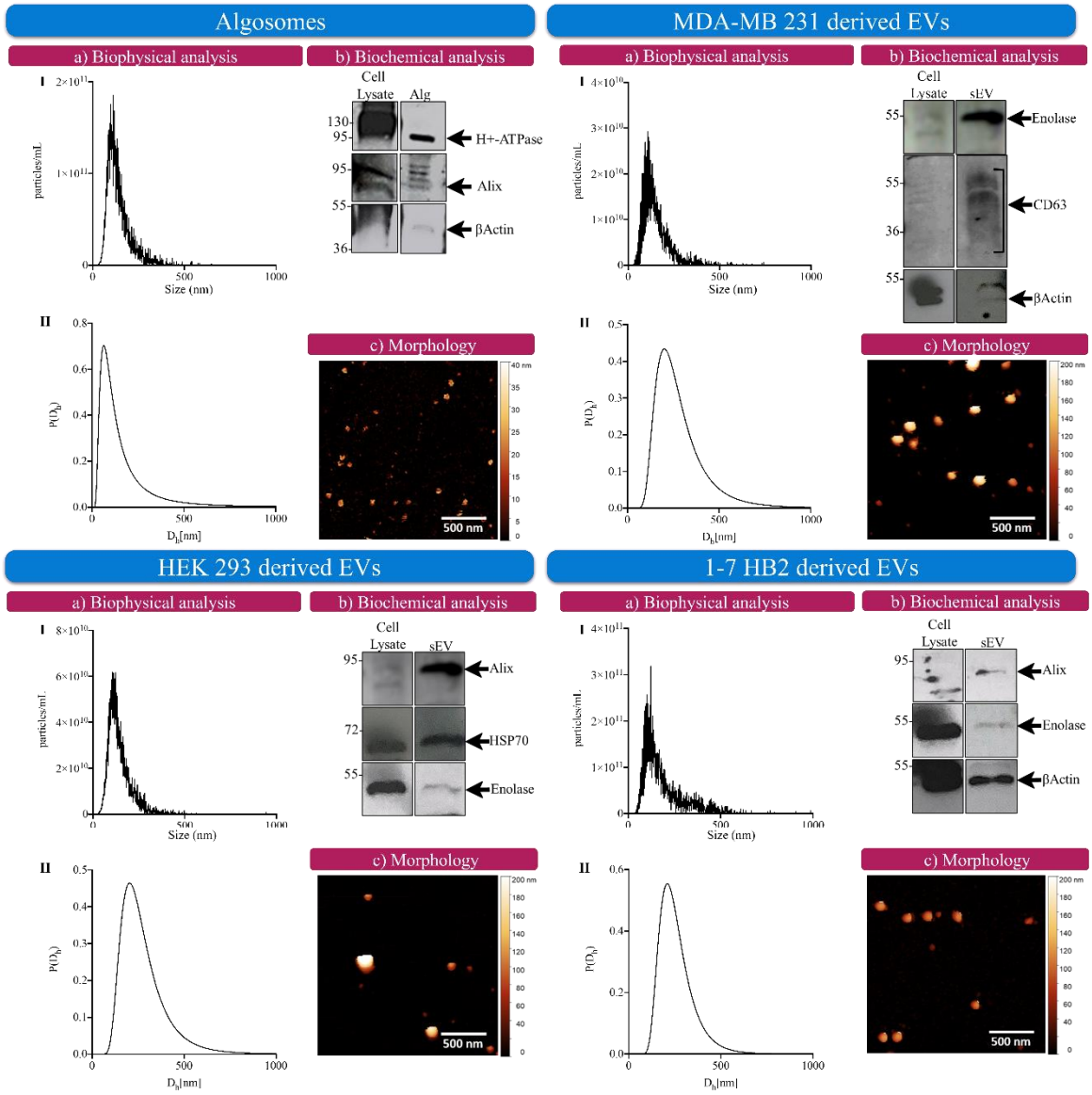

Supporting figure 1. Characterization of nanoalgosomes, MDA MB 231, HEK 293, and 1-7 HB2 derived sEVs: a) Representative biophysical analysis of the particle size distribution by (I) nanoparticles tracking analysis (NTA) and (II) dynamic light scattering (DLS) (n=3); b) Representative biochemical analysis of specific-EV biomarkers by immunoblotting on the sEVs and the respective cell lysate; c) Representative image of morphological analysis by atomic force microscopy (AFM).

- Supporting Figures –

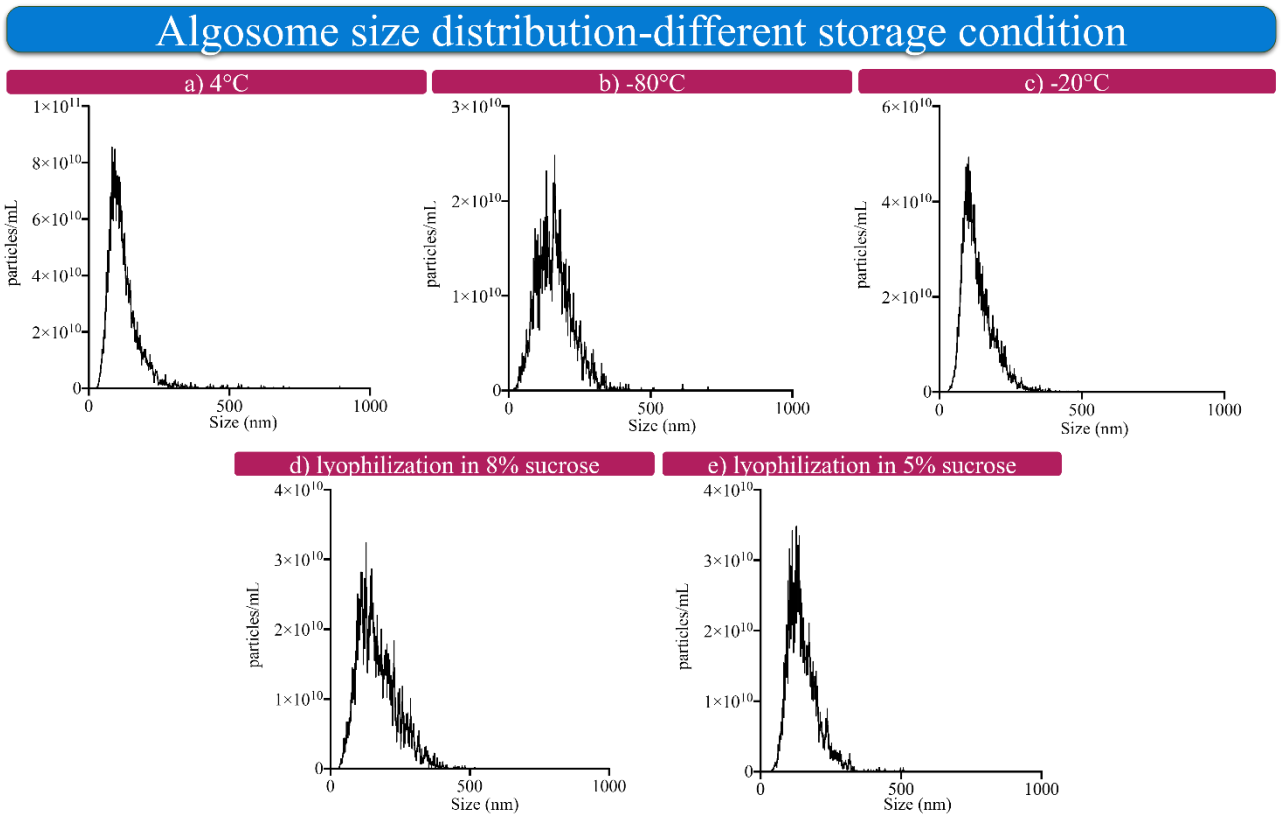

Supporting figure 2. Nanoalgosome size distribution by NTA after different storage condition: a) 4°C; b) -80°C; c) -20°C; d) lyophilization in 8% sucrose and e) lyophilization in 5% sucrose.

- Supporting Figures -

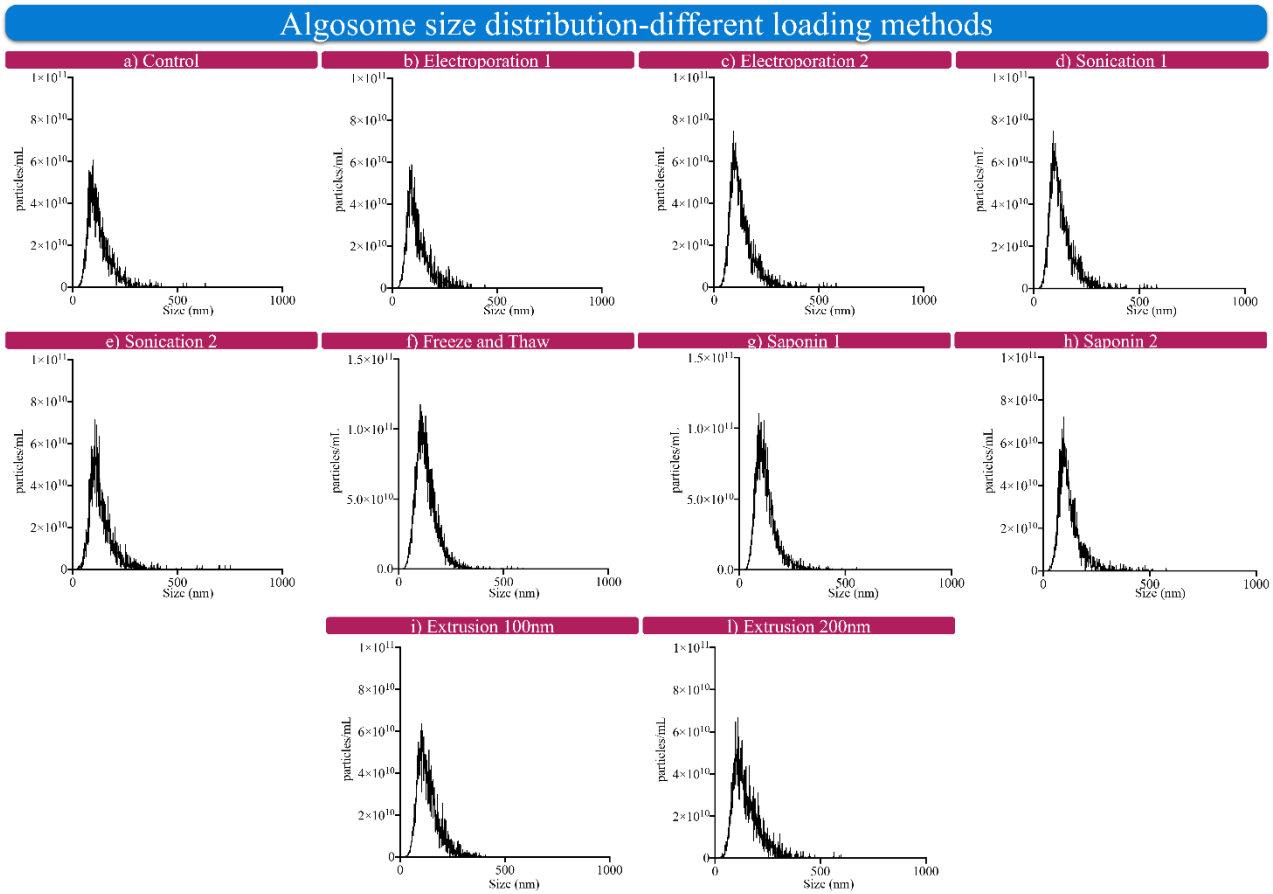

Supporting figure 3. Nanoalgosome size distribution by NTA after different loading methods a) Control; b) Electroporation 1; c) Electroporation 2; d) Sonication 1; e) Sonication 2; f) Freeze and Thaw; g) Saponin 1; h) Saponin 2; i) Extrusion 100nm and l) Extrusion 200nm.

- Supporting Methods -

Microalgae cultivation

A stock culture of the microalgae *T. chuii* (CCAP 66/21b), grown in borosilicate glass bottles was used to start new cultures in bottles via a 25% v/v inoculum. Microalgae medium are constitute of certified ultrafiltered, clear and sterile marine water (Steralmar) with Guillard′s (F/2) enrichment solution (F/2 medium). Cultures were kept for 4 weeks at a temperature of 22°C ± 2°C under continuous air flow and exposed to white light with a photoperiod of 14 h light and 10 h dark. Bottles were gently shaken every 2 days in order to homogenize the cultures. Microalgae were cultured in sterile conditions by using 0.22 μm filters at the bottle inlets. Cell growth was monitored every week by optical density at 600 nm and cell counting.

Mammalian cell cultivation

The following cell lines were used for EV production: (i) 1–7 HB2, normal mammary epithelial cells; (ii) MDA-MB 231, human breast cancer epithelial cells; and (iii) HEK 293T, human embryonic kidney cells. MDA-MB-231 and HEK293T were cultured in Dulbecco's Modified Eagle Medium (DMEM, Sigma-Aldrich) containing 10% (v/v) Fetal Bovine Serum (FBS, Gibco, Life Technologies) plus 2 mM L-glutamine, 100 U/ml Penicillin and 100 mg/ml Streptomycin (Sigma-Aldrich); instead, the 1–7 HB2 cell line was cultured in low-glucose DMEM (Sigma-Aldrich) containing 10% (v/v) Fetal Bovine Serum, plus 2 mM L-glutamine, 100 U/ml Penicillin and 100 mg/ml Streptomycin, 5 μg/ml Hydrocortisone (Sigma-Aldrich) and 10 μg/ml Bovine Insulin (Sigma-Aldrich). All cell lines were maintained at 37°C in a humidified atmosphere (5% CO_2). All cell lines were seeded in 175 cm^2 flasks until 70% confluence was reached. Next, cells were washed twice with phosphate saline buffer (PBS, Sigma- Aldrich) with Ca^{++} and Mg^{++} and cultured in appropriate medium supplemented with 10% of EV-depleted FBS. After 48 h, sEVs were isolated from each cell-conditioned medium.

Microalgae and human-derived-EV isolation

Differential ultracentrifugation. The isolation of both human cell and microalgal derived-EVs was performed by dUC, as described in Picciotto et al., 2021. Briefly, conditioned media was subjected to serial centrifugation steps at 4 °C. The first was at 300 x g for 10 min. The collected supernatant was subjected to 2,000 x g for 10 min to remove all cell debris. Large

EVs (lEVs) were separated in 50 ml eppendorf polypropylene conical tubes at 10,000 × g for 30 min at 4°C using an eppendorf rotor F34-6-38. We then collected sEVs from the supernatant into Beckman Coulter polypropylene open top tubes via centrifugation at 118,000 × g for 70 min at 4°C using a Beckman SW28 rotor. After a PBS washing step, the pellet was re-suspended in PBS without Ca^{++} and Mg^{++} for subsequent analyses.

Tangential flow filtration. Isolation of microalgal derived-EVs was performed using the KrosFlo® KR2i TFF System from Repligen (Spectrum Labs., Los Angeles, CA, USA) and three modified polyethersulfone hollow fiber membranes (S04-E65U-07-N, S04-P20-10-N and S04-E500-10-N, Spectrum Labs). Briefly, microalgae cultures were purified by microfiltration and ultra-filtration using a hollow fiber cartridge housed in the KrosFlo® KR2i, with cut-offs of 650 nm (S04-E65U-07-N, Spectrum Labs), 200 nm (S04-P20-10-N, Spectrum Labs), and 500-kDa (S04-E500-10-N, Spectrum Labs). Feed flow and transmembrane pressure (TMP) were kept constant at 450 ml/min and 0.05 bar, respectively. The small and large EVs recovered from the retentate of the 500 kDa and 200 nm cut-off TFF filter modules, respectively, were concentrated until a final volume of approximately 150 ml. Subsequently, using a smaller 500 kDa cut-off TFF filter module (C02-E500-10-N, Spectrum Labs, MicroKros) with a feed flow of 75 ml/min and a permeate flow of 2 ml/min, samples were further concentrated and diafiltrated seven times with PBS, without Ca^{++} and Mg^{++}, reaching a final volume of approximately 5 ml.

EV characterization

Nanoparticle tracking analysis (NTA). Particle concentration and size distributions of EVs were measured using an NTA instrument (NanoSight NS300, Malvern Panalytical, UK).
EV samples were diluted to generate a dilution in which 20–120 particles per frame were tracked, to obtain a concentration within the recommended measurement range (1 - 10 × 10^8 particles/ml). For each individual sample, five videos of 60 s were recorded and analyzed with detection threshold 5 and camera level 15-16. All videos were analyzed by NTA Software.

Dynamic light scattering (DLS). An aliquot of the vesicle solution was pipetted and centrifuged at 1000×g for 10 minutes at 4 °C to eliminate any dust particles. The supernatant was withdrawn using clean pipet tips , placed directly into a quartz cuvette, and incubated at 20 °C in a thermostated cell compartment of a Brookhaven BI200-SM goniometer.. The $g_2(t)$

autocorrelation function of scattered light intensity was measured at a scattering angle $\vartheta = 90°$ using a Brookhaven BI-9000 correlator. $g_2(t)$ is related to the size D_h of diffusing particles and their size distribution $P(D_h)$. The relation is given by $g_2(t) = 1 + |\beta \int P(D_h) \exp[-D(D_h)q^2 t]|^2$, where β is an instrumental parameter, $q = 4\pi\tilde{n}\lambda^{-1} \sin[\vartheta/2]$ is the scattering vector, with $\tilde{n}$ being the refractive index of the medium ($\tilde{n}$=1.3336), and $D(D_h)$ is the diffusion coefficient of a particle with a hydrodynamic diameter D_h, determined by the Stokes-Einstein relation $D(D_h) = k_B T\ [3\pi\eta D_h]^{-1}$, with T being the temperature and η the medium viscosity. The size distribution $P(D_h)$ is calculated assuming that the diffusion coefficient distribution is shaped as a Schultz distribution.Two robust parameters derived from this analysis are the z-averaged hydrodynamic diameter D_z and the polydispersity index PDI, an estimate of the distribution width.

Protein quantification and Immunoblot analysis. Microalgae lysates were prepared as described in Adamo et al, 2021; mammalian cellular lysates were prepared by RIPA buffer extraction protocol. RIPA lysis buffer was prepared based with 25 mM Tris-HCl pH 7.6, 150 mM NaCl, 1% NP-40, 1% sodium deoxycholate, 0.1% SDS, enriched with EDTA to a final concentration of 1 mM, a protease inhibitor cocktail, and a phosphatase inhibitor cocktail. After 15 minutes, the protein lysates were centrifuged at 10,000× g, for 20 min at 4 °C and the protein-rich supernatants stored at −80 °C until further processing Total protein of EV and cellular lysates was quantified using the microBCA protein assay kit (Thermo Fisher Scientific) according to the manufacturer's instructions, using bovine serum albumin (BSA) as a standard. Then, EV and lysate samples and standards were mixed with the working reagent and incubated for 1 h at 37°C. Absorbance values were measured at 562 nm, using a GloMax® Discover Microplate Reader. Next, EVs and cell lysates were separated by sodium dodecyl-sulfate polyacrylamide gel electrophoresis (SDS-PAGE) (10%). A total of 10 μg of EVs samples (in PBS) were mixed with proper volumes of 5X loading buffer (0.25 M Tris-Cl pH 6.8, 10% SDS, 50% glycerol, 0.25 M dithiothreitol (DTT), 0.25% bromophenol blue). Then, the samples were heated at 100°C for 5 minutes and loaded onto a 10% sodium dodecyl sulfate-polyacrylamide gel for electrophoretic analyses. Proteins were blotted onto polyvinylidene fluoride membranes (PVDF), which were blocked with 3% bovine serum albumin (BSA) in TBS-T solution (50 mM Tris HCl pH 8.0, 150 mM NaCl with 0.05% Tween 20) for 1 hour at room temperature. For nanoalgosome immunoblot were used the following primary antibodies: anti-H+-ATPase (dil. 1:1000 in 3% BSA/TBS-T1x, Clonality: Polyclonal,

Agrisera), anti-Alix (clone 3A9, dil. 1:150 in 3% BSA/TBS-T 1X, sc-53538. Santa Cruz), anti-ß-actin (clone AO480, dil. 1:500 in 3% BSA/TBS-T 1X, Millipore); for mammalian cell derived-EV immunoblot were used the following primary antibodies: anti-Enolase (clone A5, dil. 1:400 in 3% BSA/TBS-T1X, sc-271384. Santa Cruz), anti-CD63 tetraspanin (polyclonal, dil. 1:500 in 3% BSA/TBS-T 1X, Invitrogen), anti-HSP70 (W27,sc-24, dil. 1:150 in 3% BSA/TBS-T 1X, Santa Cruz) and anti-β-actin (AC-15, dil. 1:150 in 3% BSA/TBS-T 1X, Santa Cruz). Each primary antibody was incubated for 1 hour at room temperature. After washing, the membrane was incubated for 1 hour with secondary antibodies according to the manufacturer's instructions (horseradish peroxidase-conjugated secondary anti-mouse or anti-rabbit antibodies, Cell Signaling). The membrane was washed four times in TBS-T for 20 minutes. The immunoblots were revealed using SuperSignal Pierce ECL (Thermo Fisher Scientific).

Atomic Force Microscopy (AFM). Sample preparation: glass slides were cleaned by boiling acetone, dried by nitrogen stream and exposed to UV rays (30 W Hg lamp); then they have been i) treated with a 0.25 M (3-aminopropyl)-triethoxysilane in chloroform solution for 3 minutes, and then rinsed with chloroform and dried with nitrogen; (ii) treated with 0.4 M glutaraldehyde aqueous solution for 3 minutes and then rinsed with Milli-Q water and dried with nitrogen. The vesicle solutions diluted in PBS to a final concentration of a few μg/ml were deposited onto APTES/glutaraldehyde functionalized glass slides and incubated overnight. Then, the samples were gently rinsed by PBS to remove non-adsorbed vesicles.
Vesicle imaging: Quantitative Imaging AFM measurements were carried out in PBS by using a Nanowizard III scanning probe microscope (JPK Instruments AG, Germany) equipped with a 15-μm z-range scanner, and AC40 (Bruker) silicon cantilevers (spring constant 0.1 N/m, typical tip radius 8 nm). The images (resolution 206x206 pixels) were acquired at force setpoint 110 pN and extend speed 25 μm/s (z-length 50 nm or 80 nm and pixel time 5 ms or 8 ms respectively for algosomes and EVs from mammalian cells). The cantilever was thermally calibrated by using the tool in JPK software (Hutter and Bechhoefer, 1993).

Fluorescent-nanoparticle tracking analysis (F-NTA). EVs were stained with 500 nm of 4-(2-[6-(diethylamino)-2-naphthalenyl]ethynyl)-1-(3 sulfopropyl) pyridinium, DI-8-ANEPPS (Ex/Em: 467/631 nm, Thermo Fisher Scientific), previously filtered by 20 nm filters (Whatman Anotop filters), whose fluorescence is activated in a-polar environments, and

specifically enhanced when bound to the lipid membrane of EVs, with a higher quantum yield concerning any binding to hydrophobic protein regions.

This makes the Di-8-ANEPPS fluorescent signal highly EV-specific. After 1 h at room temperature, F-NTA analyses were carried out as described in Adamo et al., 2021.